Search for anomalous Wtb couplings and flavour-changing neutral currents in t-channel single top quark production in pp collisions at $\sqrt{s} = 7$ and $8\,\text{TeV}$

The CMS collaboration

E-mail: cms-publication-committee-chair@cern.ch

ABSTRACT: Single top quark events produced in the t channel are used to set limits on anomalous Wtb couplings and to search for top quark flavour-changing neutral current (FCNC) interactions. The data taken with the CMS detector at the LHC in proton-proton collisions at $\sqrt{s} = 7$ and $8\,\text{TeV}$ correspond to integrated luminosities of 5.0 and $19.7\,\text{fb}^{-1}$, respectively. The analysis is performed using events with one muon and two or three jets. A Bayesian neural network technique is used to discriminate between the signal and backgrounds, which are observed to be consistent with the standard model prediction. The 95% confidence level (CL) exclusion limits on anomalous right-handed vector, and left- and right-handed tensor Wtb couplings are measured to be $|f_V^R| < 0.16$, $|f_T^L| < 0.057$, and $-0.049 < f_T^R < 0.048$, respectively. For the FCNC couplings κ_{tug} and κ_{tcg}, the 95% CL upper limits on coupling strengths are $|\kappa_{\text{tug}}|/\Lambda < 4.1 \times 10^{-3}\,\text{TeV}^{-1}$ and $|\kappa_{\text{tcg}}|/\Lambda < 1.8 \times 10^{-2}\,\text{TeV}^{-1}$, where Λ is the scale for new physics, and correspond to upper limits on the branching fractions of 2.0×10^{-5} and 4.1×10^{-4} for the decays $t \to ug$ and $t \to cg$, respectively.

Contents

1 Introduction

Single top quark (t) production provides ways to investigate aspects of top quark physics that cannot be studied with $t\bar{t}$ events [1]. The theory of electroweak interactions predicts three mechanisms for producing single top quarks in hadron-hadron collisions. At leading order (LO), these are classified according to the virtuality of the W boson propagation in t-channel, s-channel, or associated tW production [2]. Single top quark production in all channels is directly related to the squared modulus of the Cabibbo-Kobayashi-Maskawa matrix element $V_{\rm tb}$. As a consequence, it provides a direct measurement of this quantity and thereby a check of the standard model (SM). The single top quark topology also opens a window for searches of anomalous Wtb couplings relative to the SM, where the interaction vertex of the top quark with the bottom quark (b) and the W boson (Wtb vertex) has a V-A axial-vector structure. Flavour-changing neutral currents (FCNC) are absent at lowest order in the SM, and are significantly suppressed through the Glashow-Iliopoulos-Maiani mechanism [3] at higher orders. Various rare decays of K, D, and B mesons, as well as the oscillations in $K^0\overline{K}^0$, $D^0\overline{D}^0$, and $B^0\overline{B}^0$ systems, strongly constrain FCNC interactions

involving the first two generations and the b quark [4]. The V-A structure of the charged current with light quarks is well established [4]. However, FCNC involving the top quark, as well as the structure of the Wtb vertex, are significantly less constrained. In the SM, the FCNC couplings of the top quark are predicted to be very small and not detectable at current experimental sensitivity. However, they can be significantly enhanced in various SM extensions, such as supersymmetry [5–7], and models with multiple Higgs boson doublets [8–10], extra quarks [11–13], or a composite top quark [14]. New vertices with top quarks are predicted, in particular, in models with light composite Higgs bosons [15, 16], extra-dimension models with warped geometry [17], or holographic structures [18]. Such possibilities can be encoded in an effective field theory through higher-dimensional gauge-invariant operators [19, 20]. Direct limits on top quark FCNC parameters have been established by the CDF [21], D0 [22], and ATLAS [23] Collaborations. There are two complementary strategies to search for FCNC in single top quark production. A search can be performed in the s channel for resonance production through the fusion of a gluon (g) with an up (u) or charm (c) quark, as was the case in analyses by the CDF and ATLAS Collaborations. However, as pointed out by the D0 Collaboration, the s-channel production rate is proportional to the square of the FCNC coupling parameter and is therefore expected to be small [22]. On the other hand, the t-channel cross section and its corresponding kinematic properties have been measured accurately at the LHC [24–26], with an important feature being that the t-channel signature contains a light-quark jet produced in association with the single top quark. This light-quark jet can be used to search for deviations from the SM prediction caused by FCNC in the top quark sector. This strategy was applied by the D0 Collaboration [22], as well as in our analysis. Models that have contributions from FCNC in the production of single top quarks can have sizable deviations relative to SM predictions. Processes with FCNC vertices in the decay of the top quark are negligible. In contrast, the modelling of Wtb couplings can involve anomalous Wtb interactions in both the production and the decay, because both are significantly affected by anomalous contributions. All these features are explicitly taken into account in the CompHEP Monte Carlo (MC) generator [27]. In this paper, we present a search by the CMS experiment at the CERN LHC for anomalous Wtb couplings and FCNC interactions of the top quark through the u or c quarks and a gluon (tug or tcg vertices), by selecting muons arising from W boson decay (including through a τ lepton) from the top quarks in muon+jets events. Separation of signal and background is achieved through a Bayesian neural network (BNN) technique [28, 29], performed using the Flexible Bayesian modelling package [30]. Limits on Wtb and top quark FCNC anomalous couplings are obtained from the distribution in the BNN discriminants.

2 The CMS detector

The central feature of the CMS apparatus is a superconducting solenoid of 6 m internal diameter, providing a magnetic field of 3.8 T. Within the solenoid volume are a silicon pixel and strip tracker, a lead tungstate crystal electromagnetic calorimeter (ECAL), and a brass and scintillator hadron calorimeter (HCAL), each composed of a barrel and two endcap sections. Forward calorimeters extend the pseudorapidity η [31] coverage provided by the

barrel and endcap detectors. Muons are measured in gas-ionization detectors embedded in the steel flux-return yoke outside the solenoid. The first level of the CMS trigger system, composed of custom hardware processors, uses information from the calorimeters and muon detectors to select the most interesting events in a fixed time interval of less than $4\,\mu\text{s}$. The high-level trigger processor farm further decreases the event rate from around $100\,\text{kHz}$ to less than $1\,\text{kHz}$, before data storage. A more detailed description of the CMS detector, together with a definition of the coordinate system used and the relevant kinematic variables, can be found in ref. [31]. The particle-flow event algorithm [32, 33] reconstructs and identifies each individual particle with an optimized combination of information from the various elements of the CMS detector. The energy of photons is directly obtained from the ECAL measurement, corrected for zero-suppression effects. The energy of electrons is determined from a combination of the electron momentum at the primary interaction vertex as determined by the tracker, the energy of the corresponding ECAL cluster, and the energy sum of all bremsstrahlung photons spatially compatible with originating from the electron track. The energy of muons is obtained from the curvature of the corresponding track. The energy of charged hadrons is determined from a combination of their momentum measured in the tracker and the matching ECAL and HCAL energy deposits, corrected for zero-suppression effects and for the response function of the calorimeters to hadronic showers. Finally, the energy of neutral hadrons is obtained from the corresponding corrected ECAL and HCAL energy. Jets are reconstructed offline from particle-flow candidates clustered by the anti-k_{T} algorithm [34, 35] with a size parameter of 0.5. Jet momentum is determined as the vectorial sum of all particle momenta in the jet, and is found from simulation to be within 5 to 10% of the true momentum over the whole transverse momentum (p_{T}) spectrum and detector acceptance. An offset correction is applied to jet energies to take into account the contribution from additional proton-proton interactions within the same or nearby bunch crossing (pileup). Jet energy corrections are derived from simulation, and are confirmed with in situ measurements of the energy balance in dijet and photon+jet events. Additional selection criteria are applied to each event to remove spurious jet-like features originating from isolated noise patterns in certain HCAL regions. The missing transverse momentum vector $\vec{p}_{\text{T}}^{\text{miss}}$ is defined as the projection on the plane perpendicular to the beams of the negative vector sum of the momenta of all reconstructed particles in an event. Its magnitude is referred to as $E_{\text{T}}^{\text{miss}}$ [32].

3   Data and simulated events

The analysis is performed using proton-proton collisions recorded with the CMS detector in 2011 and 2012 at centre-of-mass energies of 7 and $8\,\text{TeV}$, respectively, and corresponding to integrated luminosities of 5.0 and $19.7\,\text{fb}^{-1}$. The t-channel production of a single top quark is modelled using the CompHEP 4.5 package [27], supplemented by an additional matching method used to simulate an effective next-to-leading-order (NLO) approach [36]. The NLO cross sections used for t-channel single top production are $\sigma(7\,\text{TeV}) = 64.6^{+2.6}_{-1.9}\,\text{pb}$ [37] and $\sigma(8\,\text{TeV}) = 84.7^{+3.8}_{-3.2}\,\text{pb}$ [38, 39]. The POWHEG 1.0 NLO MC generator [40] provides an alternative model to estimate the sensitivity of the analysis to the modelling of the signal.

Contributions from anomalous operators are added to the CompHEP simulation for both the production and decay of top quarks. This takes into account the width of the top quark, spin correlations between the production and decay, and the b quark mass in the anomalous and SM contributions. The LO MadGraph 5.1 [41] generator is used to simulate the main background processes: top quark pair production with total cross sections of $\sigma(7\,\mathrm{TeV}) = 172.0^{+6.5}_{-7.6}\,\mathrm{pb}$ [42] and $\sigma(8\,\mathrm{TeV}) = 253^{+13}_{-14}\,\mathrm{pb}$ [43], and W boson production with total cross sections of $\sigma(7\,\mathrm{TeV}) = 31.3 \pm 1.6\,\mathrm{nb}$ and $\sigma(8\,\mathrm{TeV}) = 36.7 \pm 1.3\,\mathrm{nb}$ [44], for processes with up to 3 and 4 additional jets in the matrix element calculations, respectively. The subdominant backgrounds from Drell-Yan in association with jets (Z/γ^*+jets) production, corresponding to $\sigma(7\,\mathrm{TeV}) = 5.0 \pm 0.3\,\mathrm{nb}$ and $\sigma(8\,\mathrm{TeV}) = 4.3 \pm 0.2\,\mathrm{nb}$ [44], and from WW, WZ, and ZZ (dibosons) production, corresponding to $\sigma(7\,\mathrm{TeV}) = 67.1 \pm 1.7\,\mathrm{pb}$ and $\sigma(8\,\mathrm{TeV}) = 73.8 \pm 1.9\,\mathrm{pb}$ [45] are modelled using LO pythia 6.426 [46]. The contribution from multijet events, with one of the jets misidentified as a lepton, is estimated using a mutually exclusive data sample. The details are given in the next section. Single top quark production in the s channel with $\sigma(7\,\mathrm{TeV}) = 4.6^{+0.2}_{-0.2}\,\mathrm{pb}$, $\sigma(8\,\mathrm{TeV}) = 5.5 \pm 0.2\,\mathrm{pb}$, and in the tW channel with $\sigma(7\,\mathrm{TeV}) = 15.7 \pm 1.2\,\mathrm{pb}$, $\sigma(8\,\mathrm{TeV}) = 22.2 \pm 1.5\,\mathrm{pb}$ [47] are modelled using the powheg generator. The pythia 6.4 program is also used to simulate parton showers for the hard processes calculated in the CompHEP, MadGraph, and powheg generators. The PDF4LHC recipe [48] is used to reweight all simulated events to the central value of CT10 PDF [49]. The Z2Star [50, 51] set of parameters is used to simulate the underlying-events. Because of the importance of the W+jets background and the significant difference in the kinematic distributions, the following contributions are considered separately in the analysis: W boson produced together with a pair of b or c quarks (W+Q$\overline{\mathrm{Q}}$); W boson produced in association with a c quark (W+c); W boson events that do not contain heavy quarks (W+light); and events associated with underlying events (UE) that contain heavy quarks originating from the initial parton interaction (W+QX). Different nuisance parameters for the normalization scale factors are used for these components of the complete W+jets MadGraph simulation. Simulated events are reweighted to reproduce the observed particle multiplicity from pileup. Small differences between the data and simulation in trigger efficiency [52, 53], lepton identification and isolation [52, 53], and b tagging [54] are corrected via scale factors, which are generally close to unity.

4 Event selection

The following signature is used to identify t-channel single top quark production candidates: exactly one isolated muon [52], one light-flavour jet in the forward region (defined below); one b-tagged jet [54] from the b quark originating from the decay of the top quark, and an associated "soft" b jet. The "soft" b jet is likely to fail either the p_T or η threshold (given below). The presence of a neutrino in the decay of the W boson leads to a significant amount of $E_\mathrm{T}^\mathrm{miss}$, which is used to enhance the signal. The analysis is performed using data collected with a trigger requiring at least one muon in each event. To accommodate the increasing instantaneous luminosity delivered by the LHC in 2011, different triggers were used for various data-taking periods, with the muon p_T threshold ranging from 20 to

27 GeV. A single trigger with muon threshold $p_T > 24$ GeV was used in 2012. The selected events are required to have:

(i). at least one primary vertex reconstructed from at least four tracks, and located within 24 cm in the longitudinal direction and 2 cm in the radial direction from the centre of the detector;

(ii). only one isolated ($I_{rel}^{\mu} < 0.12$) muon [52] with $p_T > 20$ (27) GeV according to the variation of the trigger p_T threshold at $\sqrt{s} = 7$ and $p_T > 26$ GeV at $\sqrt{s} = 8$ TeV, and $|\eta| < 2.1$, originating from the primary vertex, where the relative isolation parameter of the muon, I_{rel}^{μ}, is defined as the sum of the energy deposited by long-lived charged hadrons, neutral hadrons, and photons in a cone with radius $\Delta R = \sqrt{(\Delta \eta^2 + \Delta \phi^2)} = 0.4$, divided by the muon p_T, where $\Delta \eta$ and $\Delta \phi$ are the differences in pseudorapidity and azimuthal angle (in radians), respectively, between the muon and the other particle's directions. Events with additional muons or electrons are rejected using a looser quality requirement of $p_T > 10$ GeV for muons and 15 GeV for electrons, $|\eta| < 2.5$, and having $I_{rel}^{\mu} < 0.2$ and $I_{rel}^{e} < 0.15$, where the electron relative isolation parameter I_{rel}^{e} is measured similarly to that for a muon;

(iii). two or three jets with $p_T > 30$ GeV and $|\eta| < 4.7$, and, at $\sqrt{s} = 8$ TeV, the highest-p_T jet (j$_1$) is required to satisfy $p_T(j_1) > 40$ GeV. For events with 3 jets we require the second-highest-p_T jet (j$_2$) to have $p_T(j_2) > 40$ GeV;

(iv). at least one b-tagged jet and at least one jet that fails the combined secondary vertex algorithm tight b tagging working-point requirement [54]. A tight b tagging selection corresponds to an efficiency of $\approx$50% for jets originating from true b quarks and a mistagging rate of $\approx$0.1% for other jets in the signal simulation.

Control regions containing events with 2 or 3 jets and no b-tagged jet, and events with 4 jets, 2 of which are b-tagged, are used to validate the modelling of the W+jets and t$\bar{t}$ backgrounds, respectively. The multijet events contribute background when there is a muon from the semileptonic decay of a b or c quark, or a light charged hadron is misidentified as a muon. These background muons candidates are usually surrounded by hadrons. This feature is exploited to define a control region by demanding exactly one muon with an inverted isolation criteria for hadronic activity of $0.35 < I_{rel}^{\mu} < 1$. The jets falling inside the cone of a size $\Delta R = 0.5$ around the selected muon are removed and the remaining jets are subject to the criteria that define the signal. To suppress the multijet background, we use a dedicated Bayesian neural network (multijet BNN), with the following input variables, sensitive to multijet production: the transverse mass $m_T(W) = \sqrt{2p_T(\mu)E_T^{miss}(1 - \cos[\Delta\phi(\mu, \vec{p}_T^{miss})])}$ of the reconstructed W boson, the azimuthal angle $\Delta\phi(\mu, \vec{p}_T^{miss})$ between the muon direction and $\vec{p}_T^{miss}$, the quantity E_T^{miss}, and the muon p_T. The same set of variables is used for both the $\sqrt{s} = 7$ and 8 TeV data sets, but because of the different selection criteria, different BNNs are trained for each set. In figure 1, data-to-simulation comparisons are shown for the multijet BNN discriminant and the $m_T(W)$ distributions for the $\sqrt{s} = 8$ TeV data. The predictions for the multijet BNN discriminant and $m_T(W)$ agree with the data.
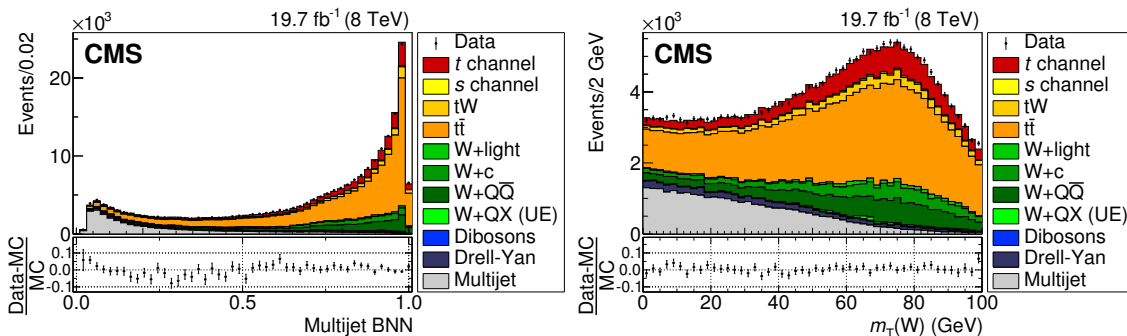
Figure 1. The distributions of the multijet BNN discriminant used for the QCD multijet background rejection (left) and the reconstructed transverse W boson mass (right) from data (points) and the predicted backgrounds from simulation (filled histograms) for $\sqrt{s} = 8\,\text{TeV}$. The lower part of each plot shows the relative difference between the data and the total predicted background. The vertical bars represent the statistical uncertainties.

	$\sqrt{s} = 7\,\text{TeV}$		$\sqrt{s} = 8\,\text{TeV}$	
Process	Basic selection	Multijet BNN > 0.7	Basic selection	Multijet BNN > 0.7
t channel	$5\,580^{+220}_{-160}$	$4\,560^{+180}_{-130}$	$21\,900^{+980}_{-840}$	$14\,800^{+660}_{-560}$
s channel	373^{+16}_{-14}	301^{+13}_{-12}	$1\,307\pm47$	865 ± 31
tW	$2\,080\pm160$	$1\,760\pm130$	$9\,220\pm620$	$6\,620\pm450$
t$\bar{\text{t}}$	$20\,450^{+770}_{-900}$	$17\,360^{+660}_{-770}$	$101\,100^{+5100}_{-6100}$	$72\,200^{+3\,600}_{-4\,300}$
W+jets	$16\,100\pm800$	$12\,700\pm630$	$36\,100^{+1200}_{-1200}$	$23\,700\pm800$
Dibosons	380 ± 10	300 ± 8	780 ± 20	537 ± 14
Drell-Yan	$1\,520\pm80$	660 ± 40	$5\,960\pm320$	$2\,060\pm110$
Multijets	$7\,340^{+3\,700}_{-3\,400}$	740^{+380}_{-350}	$30\,200^{+6\,000}_{-6\,300}$	$2\,630^{+520}_{-550}$
Total	$53\,800^{+3\,900}_{-3\,700}$	$38\,380^{+1\,000}_{-1\,100}$	$206\,650^{+8\,100}_{-8\,900}$	$123\,400^{+3\,800}_{-4\,500}$
Data	$56\,145$	$40\,681$	$222\,242$	$135\,071$

Table 1. The predicted and observed events yields before and after the multijet BNN selection for the two data sets. The uncertainties include the estimation of the scale and parton distribution function uncertainties.

The normalization of the multijet background is taken from a fit to the multijet BNN distribution, and all other processes involving a W boson are normalized to their theoretical cross sections. To reduce the multijet background, the multijet BNN discriminant is required to have a value greater than 0.7. Using the value of the discriminant rather than a selection on $m_{\text{T}}(\text{W})$ increases the signal efficiency by 10%, with a similar background rejection. This requirement rejects about 90% of the multijet background, while rejecting only about 20% of the signal, as determined from simulation. The observed and predicted event yields before and after the multijet background suppression are listed in table 1.

5 Signal extraction with Bayesian neural networks

Events that pass the initial selection and the multijet BNN discriminant requirement are considered in the final analysis, which requires the training of the BNN (SM BNN) to distinguish the t-channel single top quark production process from other SM processes. The s- and tW-channels, $t\bar{t}$, W+jets, diboson, and Drell-Yan processes with their relative normalizations are treated as a combined background for the training of the SM BNN. The SM BNN discriminant is used to remove the SM backgrounds in the search for an anomalous structure at the Wtb vertex. Three additional Wtb BNNs are used to separate the individual contributions of right-handed vector (f_V^R), left-handed (f_T^L) and right-handed (f_T^R) tensor couplings from the left-handed vector coupling (f_V^L) expected in the SM. The physical meanings of these couplings are discussed in section 7. The FCNC processes with anomalous tcg and tug vertices are assumed to be completely independent of the SM contribution. In addition tcg BNN and tug BNN are trained to distinguish the corresponding contributions from the SM contribution. The kinematic properties of the potential tcg and tug contributions are slightly different owing to the different initial states and the discussion of the couplings appears in section 8. The input variables used by each BNN are summarised in table 2. Their choice is based on the difference in the structure of the Feynman diagrams contributing to the signal and background processes. Distributions of four representative variables for data and simulated events are shown in figure 2. Several variables in the analysis require full kinematic reconstruction of the top quark and W boson candidates. For the kinematic reconstruction of the top quark, the W boson mass constraint is applied to extract the component of the neutrino momentum along the beam direction (p_z). This leads to a quadratic equation in p_z. For two real solutions of the equation, the smaller value of p_z is used as the solution. For events with complex solutions, the imaginary components are eliminated by modifying E_T^{miss} such that $m_T(W) = M_W$ [4]. The data-to-simulation comparisons shown in figure 3 demonstrate good agreement in the control regions enriched in top quark pair events (4 jets with 2 b tags) and W+jets (no b-tagged jets), as well as in the signal regions, as discussed in section 4. In figure 3, the simulated events are normalized to the results obtained in the fit to the data.

6 Systematic uncertainties and statistical analysis

The analysis extracts the parameters of single top quark production and any signs of beyond the SM behaviour based on the BNN discriminant distributions. It follows the same methodology for estimating the uncertainties as used in previously CMS measurements of single top quark production [58, 59]. Bayesian inference is used to derive the posterior probability. A signal strength $\vec{\mu}_s$ is the central value of the posterior probability distribution $p(\vec{\mu}_s|d)$ with a certain data set d. This posterior probability can be obtained as the integral

$$p(\vec{\mu}_s|d) = \int p(d|\vec{\mu}_s, \vec{\mu}_b, \vec{\theta}) \frac{\pi(\vec{\mu}_s)\pi(\vec{\mu}_b)\pi(\vec{\theta})}{\pi(d)} \mathrm{d}\vec{\mu}_b \mathrm{d}\,\vec{\theta}, \tag{6.1}$$

where $\vec{\mu}_b$ are the background yields, $\vec{\theta}$ are additional nuisance parameters, which are the systematic uncertainties of the analysis, $\pi(\vec{\mu}_s)$, $\pi(\vec{\mu}_b)$, and $\pi(\vec{\theta})$ are the prior probabili-

Variable	Description	SM	$f_V^L f_V^R$	$f_V^L f_T^L$	$f_V^L f_T^R$	FCNC
$p_T(b_1)$	p_T of the leading b jet (the b-tagged jet with the highest p_T)	×				
$p_T(b_2)$	p_T of the next-to-leading b jet	7				
$p_T(j_1)$	p_T of the leading jet			×	×	×
$p_T(j_1,j_2)$	vector sum of the p_T of the leading and the next-to-leading jet	×		×		
$p_T(\sum_{i\neq i_{\text{best}}}\vec{p_T}(j_i))$	vector sum of the p_T of all jets without the best jet	7				
$p_T(j_L)$	p_T of the light-flavour jet (untagged jet with the highest value of $|\eta|$)	×		×	×	×
$p_T(\mu)$	p_T of the muon	7	×	×		
$p_T(W,b_1)$	p_T of the W boson and the leading b jet	×		×	×	×
$H_T(j_1,j_2)$	scalar sum of the p_T of the leading and the next-to-leading jet	×		×	×	×
E_T^{miss}	missing transverse energy		×			
$\eta(\mu)$	η of the muon	×				
$\eta(j_L)$	η of the light-flavour jet	×		×		×
$M(j_1,j_2)$	invariant mass of the leading and the next-to-leading jets	×		×	×	×
$M(\sum_{i\neq i_{\text{best}}}(j_i))$	invariant mass of all jets without the best one	7				
$M(jW)$	invariant mass of the W boson and all jets	×			×	×
$M(W,b_1)$	invariant mass of the W boson and the leading b jet	×				
$\Delta R(\mu,b_1)$	$\sqrt{(\eta(\mu)-\eta(b_1))^2+(\phi(\mu)-\phi(b_1))^2}$				8	
$\Delta R(\mu,j_1)$	$\sqrt{(\eta(\mu)-\eta(j_1))^2+(\phi(\mu)-\phi(j_1))^2}$				7	
$\Delta\phi(\mu,E_T^{\text{miss}})$	azimuthal angle between the muon and $\vec{p}_T^{\text{miss}}$		×	×		
$\Delta\phi(\mu,W)$	azimuthal angle between the muon and the W boson		8			
$\cos(\theta_{\mu,j_L})|_{\text{top}}$	cosine of the angle between the muon and the light-flavour jet in the top quark rest frame, for top quark reconstructed with the leading b jet [55]	×	×		7	×
$\cos(\theta_{\mu,W})|_{W}$	cosine of the angle between the muon momentum in the W boson rest frame and the direction of the W boson boost vector [56]	×	×	×		
$\cos(\theta_{W,j_L})|_{\text{top}}$	cosine of the angle between the W boson and the light-flavour jet in the top quark rest frame [56]	8	×			
$Q(\mu)$	charge of the muon					tug
Planarity	measure of the flatness of the event using the smallest eigenvalue of the normalized momentum tensor [57]	8				
SM BNN	SM BNN discriminant					×

Table 2. Input variables for the BNNs used in the analysis. The symbol × represents the variables used for each particular BNN. The number 7 or 8 marks the variables used in just the $\sqrt{s}=7$ or 8 TeV analysis. The symbol "tug" marks the variables used just in the training of the tug FCNC BNN. The notations "leading" and "next-to-leading" refer to the highest-p_T and second-highest-p_T jet, respectively. The notation "best" jet is used for the jet that gives a reconstructed mass of the top quark closest to the value of 172.5 GeV, which is used in the MC simulation.
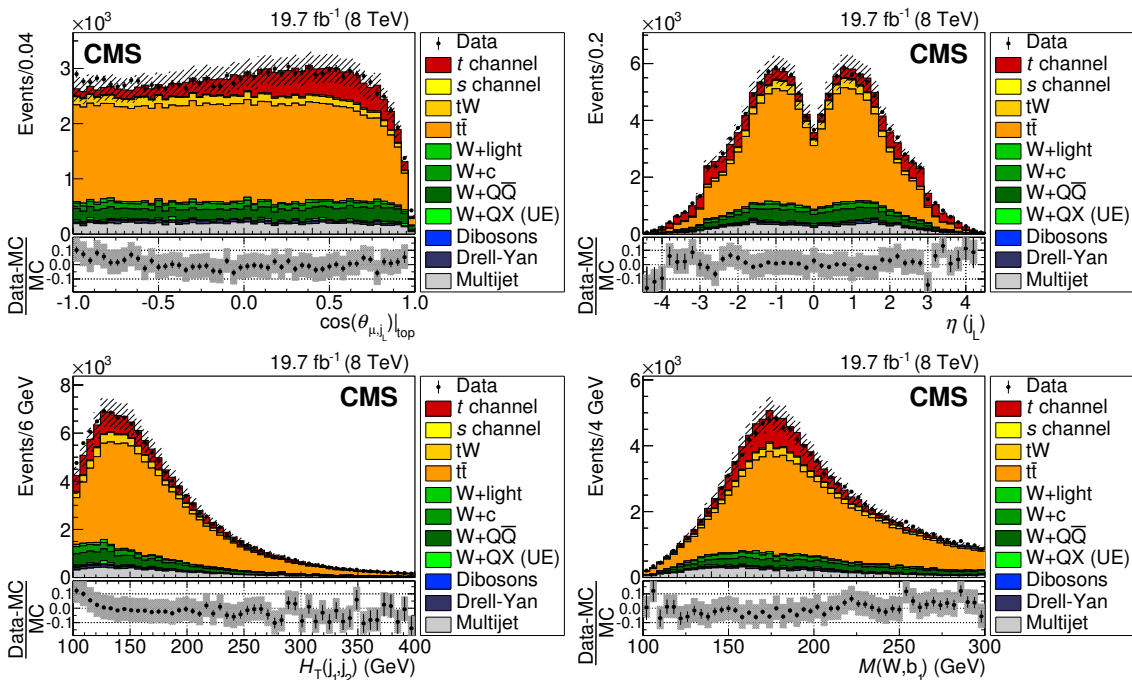
Figure 2. Comparison of experimental with simulated data of the BNNs input variables $\cos(\theta_{\mu,j_L})|_{top}$, $\eta(j_L)$, $H_T(j_1,j_2)$, and $M(W,b_1)$. The variables are described in table 2. The lower part of each plot shows the relative difference between the data and the total predicted background. The hatched band corresponds to the total simulation uncertainty. The vertical bars represent the statistical uncertainties. Plots are for the $\sqrt{s} = 8\,\text{TeV}$ data set.

ties of the corresponding parameters, $\pi(d)$ is a normalization factor, and $p(d|\vec{\mu}_s, \vec{\mu}_b, \vec{\theta})$ is the probability to obtain a given d with given $\vec{\mu}_s$, $\vec{\mu}_b$, and $\vec{\theta}$. Uncertainties considered in the analysis are discussed next. For the variation of the background normalization, scale parameters are introduced in the statistical model, and the corresponding variations of these parameters are the same as for the SM measurement in ref. [59]. All background processes and their normalizations are treated as being statistically independent. To estimate the uncertainty in the multijet distributions, two different isolation criteria are used $(0.3 < I^\mu_{rel} < 0.5$ and $0.5 < I^\mu_{rel} < 1)$. Also, a comparison is made between data and events generated with the PYTHIA 6.4 simulation. The impact of the changes in the multijet template are well within the range of -50% to $+100\%$, and this is included as a prior uncertainty in the statistical model. To estimate the uncertainties in the detector-related jet and E^{miss}_T corrections, the four-momenta of all reconstructed jets in simulated events are scaled simultaneously in accordance with p_T- and η-dependent jet energy correction (JEC) uncertainties [60]. These changes are also propagated to E^{miss}_T. The effect of the 10% uncertainty in E^{miss}_T coming from unclustered energy deposits in the calorimeters that are not associated with jets is estimated after subtracting all the jet and lepton energies from the E^{miss}_T calculation. Parameters in the procedure to correct the jet energy resolution (JER) are varied within their uncertainties, and the procedure is repeated for all jets in the simulation [60, 61]. The variations coming from the uncertainty in the b quark tagging
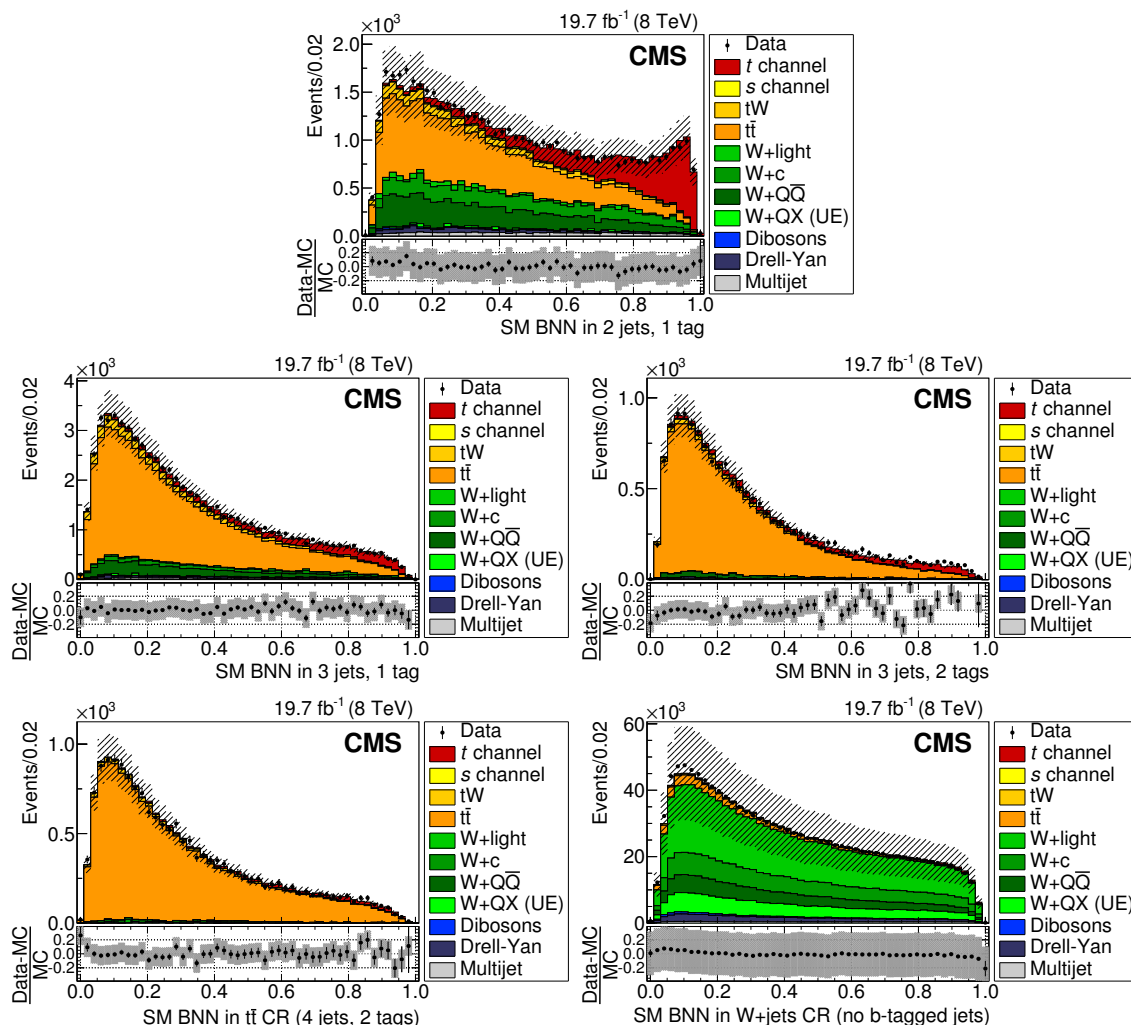
Figure 3. Comparison of $\sqrt{s} = 8$ TeV data and simulation using the SM BNN discriminant in three separate signal regions of two jets with one b-tagged (2 jets, 1 tag) (upper), three jets with one of them b-tagged (3 jets, 1 tag) (middle left), and three jets with two of them b-tagged (3 jets, 2 tags) (middle right), and in $t\bar{t}$ (4 jets, 2 tags) (lower left) and W+jets (no b-tagged jets) (lower right) background control regions (CR). The lower part of each plot shows the relative difference between the data and the total predicted background. The hatched band corresponds to the total simulation uncertainty. The vertical bars represent the statistical uncertainties.

efficiency and mistagging rate of jets are propagated to the simulated events [54]. The uncertainties for c quark jets are assumed to be twice as large as for b quark jets. The scale factors for tagging b and c quark jets are treated as fully correlated, whereas the mistagging scale factors are varied independently. The integrated luminosity in the $\sqrt{s} = 7$ and 8 TeV data-taking periods is measured with a relative uncertainty of 2.2% [62] and 2.6% [63], respectively. In the combined fits, all experimental uncertainties, including these from the integrated luminosity, are treated as uncorrelated between the data sets. The uncertainty in the pileup modelling is estimated by using different multiplicity distributions obtained

by changing the minimum-bias cross section by $\pm 5\%$ [64]. Trigger scale factors, muon identification, and muon isolation uncertainties are introduced in the statistical model as additional factors, Gaussian-distributed parameters with a mean of 1 and widths of 0.2%, 0.5%, and 0.2%, respectively. The uncertainties from additional hard-parton radiation and the matching of the samples with different jet multiplicity are evaluated by doubling or halving the threshold for the MadGraph jet-matching procedure for the top quark pair and W+jets production, using dedicated MadGraph samples generated with such shifts in the parameters [65]. The renormalization and factorization scale uncertainties are estimated using MC simulated samples generated by doubling or halving the renormalization and factorization scales for the signal and the main background processes. Uncertainties in the parton distribution functions (PDF) are evaluated with the CT10 PDF set according to the PDF4LHC formulae for Hessian-based sets. We follow this recommendation and reweight the simulated events to obtain the uncertainty, which is about 5% on average. The uncertainty from the choice of the event generator to model the signal is estimated using pseudo-experiments. These pseudo-experiments are used to fit simulated events, obtained from the CompHEP signal sample, and from the powheg signal sample. Half of the difference between these two measurements is taken as the uncertainty (5%). Previous CMS studies [66, 67] of top quark pair production showed a softer p_T distribution of the top quark in the data than predicted by the NLO simulation. A correction for the simulation of $t\bar{t}$ production background is applied. The small effect of this reweighting procedure (0.8%) is taken into account as an uncertainty. The uncertainty owing to the finite size of the simulated samples is taken into account through the Barlow-Beeston method [68]. The BNN discriminant distributions can be affected by different types of systematic uncertainties. Some of these only impact the overall normalization, while others change the shape of the distribution. Both types of systematic uncertainties are included in the statistical model through additional nuisance parameters. Systematic uncertainties related to the modelling of JEC, JER, b tagging and mistagging rates, E_T^{miss}, and pileup, are included as nuisance parameters in the fit. The variations in these quantities leads to a total uncertainty of about 6%. Other systematic uncertainties, i.e. those related to the signal model, renormalization and factorization scales, matching of partons to final jets, and choice of PDF, are handled through the pseudo-experiments to determine the difference between the varied and the nominal result. The total uncertainty from these sources is about 8%. We include uncertainties in the statistical model by following the same approach as described in previous CMS measurements of the single top quark t-channel cross section [24, 58, 59]. The SM BNN discriminant distribution after the statistical analysis and evaluation of all the uncertainties are shown in figure 4 for the two data sets. As the $\sqrt{s} = 7$ and $8\,\mathrm{TeV}$ data sets have similar selection criteria, reweighting, and uncertainties and the physics is expected to also be similar, the data sets are combined by performing a joint fit. The previously described systematic uncertainties and methods of statistical analysis are used in the combination. In the statistical model, the experimental uncertainties are treated as uncorrelated between the data sets. The theoretical uncertainties (from the choice of generator, scales, and PDF) are treated as fully correlated between the data sets. The sensitivity of the separate $\sqrt{s} = 7$ and $8\,\mathrm{TeV}$ analyses and their combination is limited by
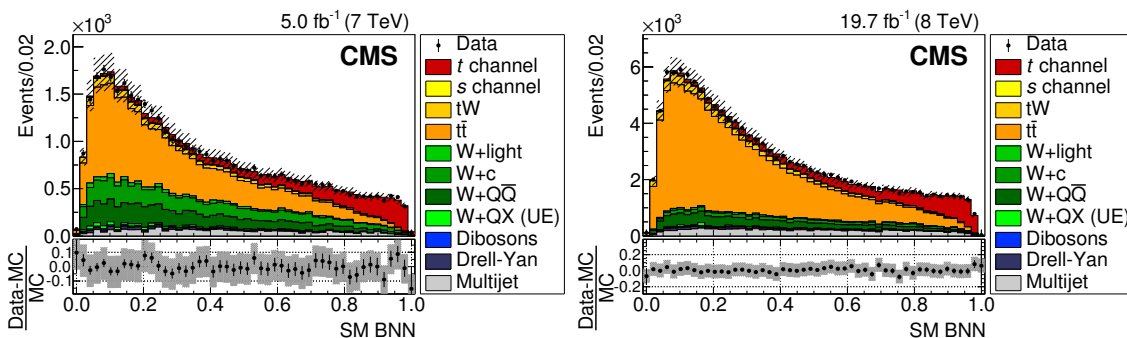
Figure 4. The SM BNN discriminant distributions after the statistical analysis and evaluation of all the uncertainties. The lower part of each plot shows the relative difference between the data and the total predicted background. The hatched band corresponds to the total simulation uncertainty. The vertical bars represent the statistical uncertainties. The left (right) plot corresponds to $\sqrt{s} = 7$ (8) TeV.

their corresponding systematic uncertainties. Therefore, the combined statistical model does not necessarily provide the tightest exclusion limits. In order to validate the analysis strategy and the statistical treatment of the uncertainties, we measure the cross sections in the SM t channel, and find values and uncertainties in agreement with previous measurements [58, 59] and with the prediction of the SM.

7 Search for anomalous contributions to the Wtb vertex

7.1 Modelling the structure of the anomalous Wtb vertex

The t-channel single top quark production is sensitive to possible deviations from the SM prediction for the Wtb vertex. The most general, lowest-dimension, CP-conserving Lagrangian for the Wtb vertex has the following form [69, 70]:

$$\mathfrak{L} = \frac{g}{\sqrt{2}}\bar{b}\gamma^{\mu}\left(f_V^L P_L + f_V^R P_R\right) t W_{\mu}^{-} - \frac{g}{\sqrt{2}}\bar{b}\frac{\sigma^{\mu\nu}\partial_{\nu}W_{\mu}^{-}}{M_W}\left(f_T^L P_L + f_T^R P_R\right) t + \text{h.c.}, \qquad (7.1)$$

where $P_{L,R} = (1 \mp \gamma_5)/2$, $\sigma_{\mu\nu} = i(\gamma_\mu\gamma_\nu - \gamma_\nu\gamma_\mu)/2$, g is the coupling constant of the weak interaction, the form factor f_V^L (f_V^R) represents the left-handed (right-handed) vector coupling, and f_T^L (f_T^R) represents the left-handed (right-handed) tensor coupling. The SM has the following set of coupling values: $f_V^L = V_{tb}, f_V^R = f_T^L = f_T^R = 0$. The same analysis scheme proposed in refs. [71, 72] is used to look for possible deviations from the SM, by postulating the presence of a left-handed vector coupling. Two of the four couplings are considered simultaneously in two-dimensional scenarios: (f_V^L, f_V^R) and (f_V^L, f_T^L), where the couplings are allowed to vary from 0 to $+\infty$, and (f_V^L, f_T^R) with variation bounds from $-\infty$ to $+\infty$. Then, considering three couplings simultaneously leads to the three-dimensional scenarios (f_V^L, f_T^L, f_T^R) and (f_V^L, f_V^R, f_T^R). In these scenarios, the couplings have the same variation range of $(0; +\infty)$ for f_V^R and f_T^L, and $(-\infty; +\infty)$ for f_V^L and f_T^R. In the presence of anomalous Wtb couplings in both the production and decay of

the top quark, the kinematic and angular distributions are significantly affected relative to their SM expectations. It is therefore important to correctly model the kinematics of such processes. Following the method of ref. [73], the event samples with left-handed (SM) interactions and a purely right-handed vector (left-handed tensor) interactions are generated to model the (f_V^L, f_V^R) $((f_V^L, f_T^L))$ scenario. Simulated event samples with the left-handed interaction in the production and the right-handed vector (left-handed tensor) interaction in the decay of the top quark, and vice versa, are also generated. The scenarios with f_T^R couplings are more complicated because of the presence of cross terms, such as $(f_V^L \cdot f_T^R)$, in the squared matrix element describing the single top quark production process. Special event samples are generated for such scenarios. Owing to the presence of the cross terms with odd power of f_V^L and f_T^R couplings, the analysis is sensitive to negative values of these couplings. The details of the simulation approach are provided in ref. [73]. All signal samples are simulated at NLO precision following ref. [36].

7.2 Exclusion limits on anomalous couplings

Following the strategy described in section 5, in addition to the SM BNN, the anomalous Wtb BNNs are trained to distinguish possible right-handed vector or left-/right-handed tensor structures from the SM left-handed vector structure in the t-channel single top quark events. The set of variables chosen for the different Wtb BNNs are listed in table 2. The first two-dimensional scenario considers a possible mixture of f_V^L and (anomalous) f_V^R couplings. The corresponding Wtb BNN (f_V^L, f_V^R) is trained to distinguish the contribution of these two couplings. For the (f_V^L, f_T^L) scenario, another Wtb BNN is trained to separate the left-handed vector interacting single top quark SM events from events with a left-handed tensor operator in the Wtb vertex. For the third scenario, (f_V^L, f_T^R), the last Wtb BNN is trained to separate left-handed-vector-interacting single top quark SM events from events with a right-handed-tensor operator in the Wtb vertex. Figure 5 shows the comparison between the data and simulation for the outputs of the Wtb BNN (f_V^L, f_V^R), Wtb BNN (f_V^L, f_T^L), and Wtb BNN (f_V^L, f_T^R). The SM BNN and one of the Wtb BNN discriminants are used as inputs in the simultaneous fit of the two BNN discriminants. One-dimensional constraints on the anomalous parameters are obtained by integrating over the other anomalous parameter in the corresponding scenario. The results of the fits are presented in the form of two-dimensional contours at 68% and 95% CL exclusion limits, and as given in table 3, as one-dimensional constraints in different scenarios. Both the one- and two-dimension limits are measured for the individual data sets and their combination. The combined observed and expected two-dimensional contours in the (f_V^L, f_V^R), (f_V^L, f_T^L), and (f_V^L, f_T^R) spaces are shown in figure 6. As the interference terms between f_T^L and f_T^R or f_V^R and f_T^R couplings are negligible [20], it is possible to consider three-dimensional scenarios with simultaneous variation of f_V^L, f_T^L, f_T^R or f_V^L, f_V^R, f_T^R couplings. The three-dimensional statistical analysis is performed using the SM BNN, Wtb BNN (f_V^L, f_T^R), and either the Wtb BNN (f_V^L, f_T^L) or Wtb BNN (f_V^L, f_V^R) discriminants to obtain the excluded regions at 68% and 95% CL for f_T^L and f_T^R, again by integrating over the other anomalous couplings. The combined $\sqrt{s} = 7$ and 8 TeV results in the three-dimensional simultaneous fit of f_V^L, f_T^L, and f_T^R couplings are presented in figure 7 (left) in the form of observed and expected 68% and
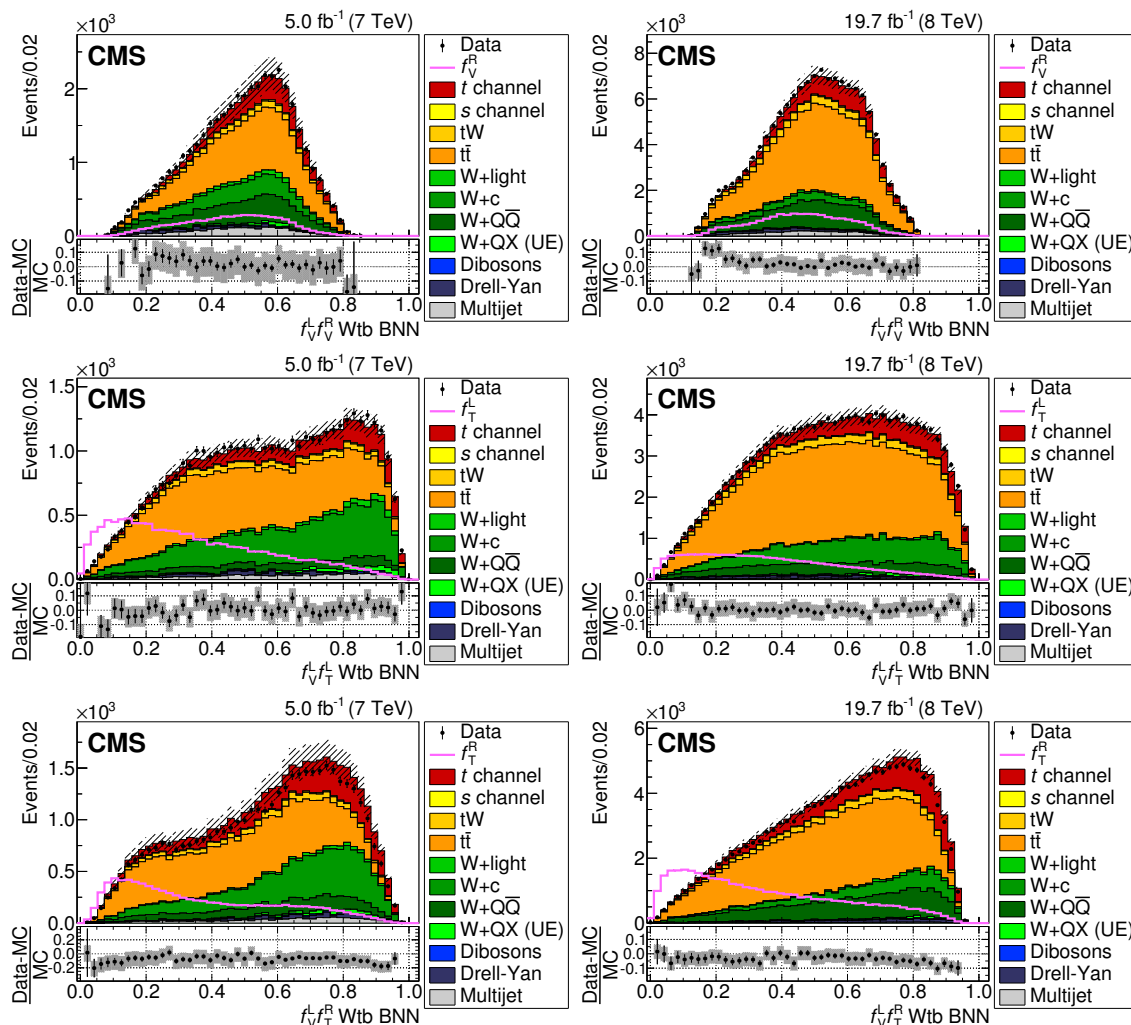
Figure 5. Distributions of the Wtb BNN discriminants from data (points) and simulation (filled histograms) for the scenarios (f_V^L, f_V^R) (top), (f_V^L, f_T^L) (middle), and (f_V^L, f_T^R) (bottom). The plots on the left (right) correspond to $\sqrt{s} = 7$ (8) TeV. The Wtb BNNs are trained to separate SM left-handed interactions from one of the anomalous interactions. In each plot, the expected distribution with the corresponding anomalous coupling set to 1.0 is shown by the solid curve. The lower part of each plot shows the relative difference between the data and the total predicted background. The hatched band corresponds to the total simulation uncertainty. The vertical bars represent the statistical uncertainties.

95% exclusion contours on the (f_T^L, f_T^R) couplings. The corresponding results for the f_V^L, f_V^R, and f_T^R couplings are shown in figure 7 (right) as two-dimensional exclusion limits in the (f_V^R, f_T^R) plane. The measured exclusion limits from the three-dimensional fits with the combined data sets are $f_V^L > 0.98$, $|f_V^R| < 0.16$, and $|f_T^L| < 0.057$. For f_T^R we take the more-conservative limits from the three-dimensional fits of $-0.049 < f_T^R < 0.048$ as our measurement. These limits are much more restrictive than those obtained by the D0 Collaboration in a direct search [72], and agree well with the recent results obtained by the ATLAS [74] and CMS [75, 76] experiments from measurements of the W boson helicity fractions.

Figure 6. Combined $\sqrt{s} = 7$ and $8\,\mathrm{TeV}$ observed and expected exclusion limits in the two-dimensional planes $(f_V^L, |f_V^R|)$ (top-left), $(f_V^L, |f_T^L|)$ (top-right), and (f_V^L, f_T^R) (bottom) at 68% and 95% CL.
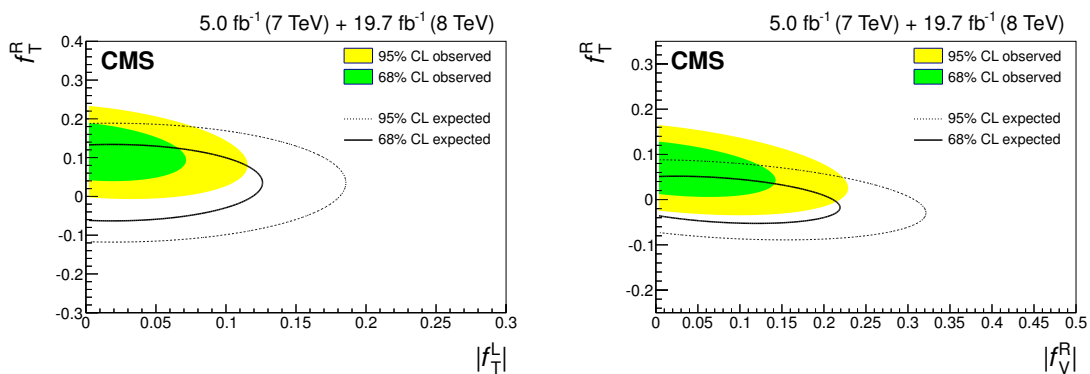

Figure 7. Combined $\sqrt{s} = 7$ and $8\,\mathrm{TeV}$ results from the three-dimensional variation of the couplings of f_V^L, f_T^L, f_T^R (left), and f_V^L, f_V^R, f_T^R (right) in the form of observed and expected exclusion limits at 68% and 95% CL in the two-dimension planes $(|f_T^L|, f_T^R)$ (left) and $(|f_V^R|, f_T^R)$ (right).

– 15 –

Scenario	$f_V^L >$	$|f_V^R| <$	$|f_T^L| <$	$< f_T^R <$	
$\sqrt{s} = 7$ TeV					
(f_V^L, f_V^R)	0.96 (0.91)	0.29 (0.37)			
(f_V^L, f_T^L)	0.88 (0.89)		0.11 (0.16)		
(f_V^L, f_T^R)	0.94 (0.91)			-0.077 (-0.067)	0.046 (0.053)
(f_V^L, f_T^L, f_T^R)	0.95 (0.91)		0.16 (0.22)	-0.074 (-0.065)	0.037 (0.055)
(f_V^L, f_V^R, f_T^R)	0.94 (0.89)	0.24 (0.29)		-0.087 (-0.076)	0.040 (0.064)
$\sqrt{s} = 8$ TeV					
(f_V^L, f_V^R)	0.96 (0.92)	0.24 (0.29)			
(f_V^L, f_T^L)	0.91 (0.92)		0.15 (0.18)		
(f_V^L, f_T^R)	0.92 (0.92)			-0.041 (-0.050)	0.060(0.048)
(f_V^L, f_T^L, f_T^R)	0.93 (0.94)		0.070(0.12)	-0.049 (-0.067)	0.080 (0.066)
(f_V^L, f_V^R, f_T^R)	0.95 (0.95)	0.18 (0.20)		-0.035 (-0.044)	0.043 (0.032)
$\sqrt{s} = 7$ and 8 TeV					
(f_V^L, f_V^R)	0.97 (0.92)	0.28 (0.31)			
(f_V^L, f_T^L)	0.92 (0.92)		0.10 (0.14)		
(f_V^L, f_T^R)	0.94 (0.93)			-0.046 (-0.050)	0.046 (0.041)
(f_V^L, f_T^L, f_T^R)	0.98 (0.97)		0.057 (0.10)	-0.049 (-0.051)	0.048 (0.046)
(f_V^L, f_V^R, f_T^R)	0.98 (0.97)	0.16 (0.22)		-0.049 (-0.049)	0.039 (0.037)

Table 3. One-dimensional exclusion limits obtained in different two- and three-dimensional fit scenarios. The first column shows the couplings allowed to vary in the fit, with the remaining couplings set to the SM values. The observed (expected) 95% CL limits for each of the two data sets and their combination are given in the following columns.

8 Search for tcg and tug FCNC interactions

8.1 Theoretical introduction

The FCNC tcg and tug interactions can be written in a model-independent form with the following effective Lagrangian [1]:

$$\mathfrak{L} = \frac{\kappa_{\mathrm{tqg}}}{\Lambda} g_s \overline{\mathrm{q}} \sigma^{\mu\nu} \frac{\lambda^{\mathrm{a}}}{2} \mathrm{t} G_{\mu\nu}^{\mathrm{a}}, \tag{8.1}$$

where Λ is the scale of new physics (≈ 1 TeV), q refers to either the u or c quarks, κ_{tqg} defines the strength of the FCNC interactions in the tug or tcg vertices, $\lambda^{\mathrm{a}}/2$ are the generators of the SU(3) colour gauge group, g_s is the coupling constant of the strong interaction, and $G_{\mu\nu}^{\mathrm{a}}$ is a gluon field strength tensor. The Lagrangian is assumed to be symmetric
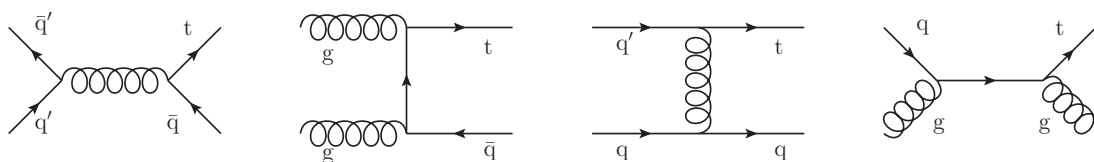
Figure 8. Representative Feynman diagrams for the FCNC processes.

with respect to the left and right projectors. Single top quark production through FCNC interactions contains 48 subprocesses for both the tug and tcg channels, and the cross section is proportional to $(\kappa_{\mathrm{tqg}}/\Lambda)^2$. Representative Feynman diagrams for the FCNC processes are shown in figure 8. Since the influence of the FCNC parameters on the total top quark width is negligible for the allowed region of FCNC parameters, the SM value for the top quark width is used in this analysis. The COMPHEP generator is used to simulate of the signal tug and tcg processes. The FCNC samples are normalized to the NLO cross sections using a K factor of 1.6 for higher-order QCD corrections [77].

8.2 Exclusion limits on tug and tcg anomalous couplings

FCNC processes are kinematically different from any SM processes, therefore, it is reasonable to train a new BNN to discriminate between FCNC production as the signal and the SM background, including the t-channel single top quark production. Owing to the possible presence of a FCNC tug or tcg signal, two BNNs are trained to distinguish each of the couplings. The variable choices for these BNNs, shown in table 2, are motivated by analysis of the Feynman diagrams of the FCNC and SM processes. The comparison of the neural network output for the data and model is shown in figure 9. Output histograms from the tug and tcg FCNC BNN discriminants for the SM backgrounds are used as input to the analysis. The posterior probability distributions of $|\kappa_{\mathrm{tug}}|/\Lambda$ and $|\kappa_{\mathrm{tcg}}|/\Lambda$ are obtained by fitting the histograms. The combined $\sqrt{s} = 7$ and 8 TeV observed and expected exclusion limits at 68% and 95% CL on the anomalous FCNC parameters in the form of two-dimensional contours are shown in figure 10. The two-dimensional contours reflect the possible simultaneous presence of the two FCNC parameters. Individual exclusion limits on $|\kappa_{\mathrm{tug}}|/\Lambda$ are obtained by integrating over $|\kappa_{\mathrm{tcg}}|/\Lambda$ and vice versa. These individual limits can be used to calculate the upper limits on the branching fractions $\mathcal{B}(\mathrm{t} \to \mathrm{ug})$ and $\mathcal{B}(\mathrm{t} \to \mathrm{cg})$ [78]. The observed and expected exclusion limits at 95% CL on the FCNC couplings and the corresponding branching fractions are given in table 4. These limits are significantly better than those obtained by the D0 [22] and CDF [21] experiments, and in previous CMS results, and are comparable to recent ATLAS measurements [23].

9 Summary

A direct search for model-independent anomalous operators in the Wtb vertex and FCNC couplings has been performed using single top quark t-channel production in data collected by the CMS experiment in pp collisions at $\sqrt{s} = 7$ and 8 TeV. Different possible
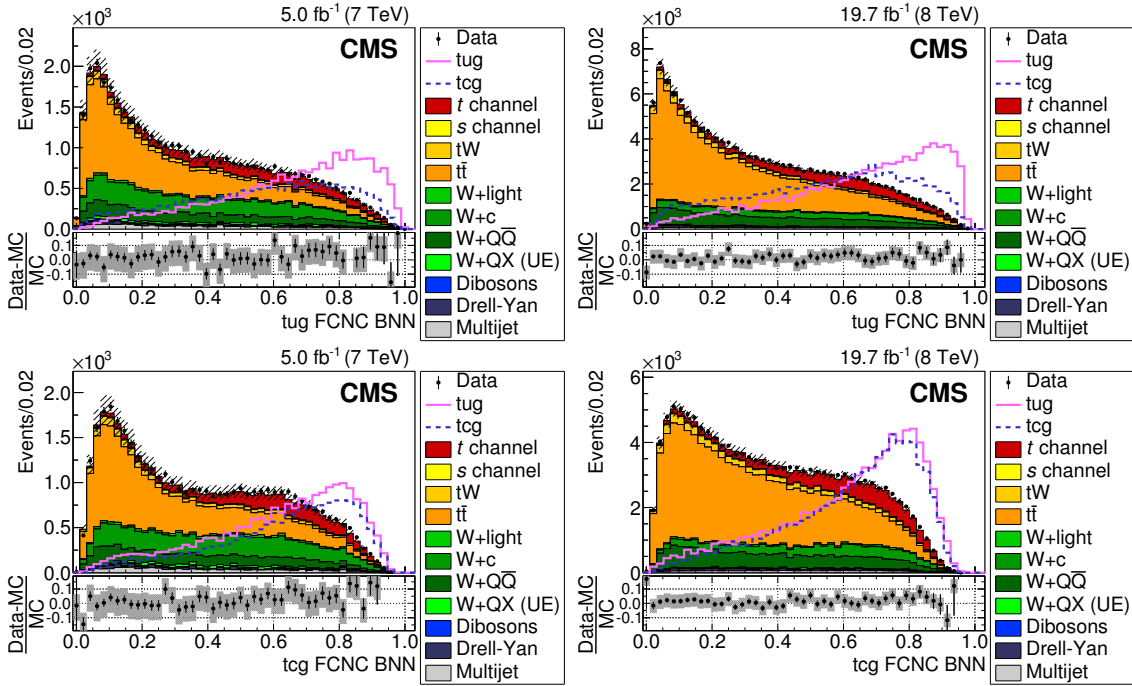
Figure 9. The FCNC BNN discriminant distributions when the BNN is trained to distinguish t → ug (upper) or t → cg (lower) processes as signal from the SM processes as background. The results from data are shown as points and the predicted distributions from the background simulations by the filled histograms. The plots on the left (right) correspond to the $\sqrt{s} = 7$ (8) TeV data. The solid and dashed lines give the expected distributions for t → ug and t → cg, respectively, assuming a coupling of $|\kappa_{\mathrm{tug}}|/\Lambda = 0.04$ (0.06) and $|\kappa_{\mathrm{tcg}}|/\Lambda = 0.08$ (0.12) TeV^{-1} on the left (right) plots. The lower part of each plot shows the relative difference between the data and the total predicted background. The hatched band corresponds to the total simulation uncertainty. The vertical bars represent the statistical uncertainties.

Figure 10. Combined $\sqrt{s} = 7$ and 8 TeV observed and expected limits for the 68% and 95% CL on the $|\kappa_{\mathrm{tug}}|/\Lambda$ and $|\kappa_{\mathrm{tcg}}|/\Lambda$ couplings.

$\sqrt{s}$	$|\kappa_{\text{tug}}|/\Lambda\ (\text{TeV}^{-1})$	$\mathcal{B}(\text{t} \rightarrow \text{ug})$	$|\kappa_{\text{tcg}}|/\Lambda\ (\text{TeV}^{-1})$	$\mathcal{B}(\text{t} \rightarrow \text{cg})$
7 TeV	14 (13) $\times 10^{-3}$	24 (21)$\times 10^{-5}$	2.9 (2.4) $\times 10^{-2}$	10.1 (6.9)$\times 10^{-4}$
8 TeV	5.1 (5.9) $\times 10^{-3}$	3.1 (4.2)$\times 10^{-5}$	2.2 (2.0) $\times 10^{-2}$	5.6 (4.8)$\times 10^{-4}$
7 and 8 TeV	4.1 (4.8) $\times 10^{-3}$	2.0 (2.8)$\times 10^{-5}$	1.8 (1.5) $\times 10^{-2}$	4.1 (2.8)$\times 10^{-4}$

Table 4. Observed (expected) upper limits at 95% CL for the FCNC couplings and branching fractions obtained using the $\sqrt{s} = 7$ and 8 TeV data, and their combination.

anomalous contributions are investigated. The observed event rates are consistent with the SM prediction, and exclusion limits are extracted at 95% CL. The combined limits in three-dimensional scenarios on possible Wtb anomalous couplings are $f_V^L > 0.98$ for the left-handed vector coupling, $|f_V^R| < 0.16$ for the right-handed vector coupling, $|f_T^L| < 0.057$ for the left-handed tensor coupling, and $-0.049 < f_T^R < 0.048$ for the right-handed tensor coupling. For FCNC couplings of the gluon to top and up quarks (tug) or top and charm quarks (tcg), the 95% CL exclusion limits on the coupling strengths are $|\kappa_{\text{tug}}|/\Lambda < 4.1 \times 10^{-3}\,\text{TeV}^{-1}$ and $|\kappa_{\text{tcg}}|/\Lambda < 1.8 \times 10^{-2}\,\text{TeV}^{-1}$ or, in terms of branching fractions, $\mathcal{B}(\text{t} \rightarrow \text{ug}) < 2.0 \times 10^{-5}$ and $\mathcal{B}(\text{t} \rightarrow \text{cg}) < 4.1 \times 10^{-4}$.

Acknowledgments

References

[1] M. Beneke et al., *Top quark physics*, `hep-ph/0003033` [inSPIRE].

[2] S.S.D. Willenbrock and D.A. Dicus, *Production of heavy quarks from W gluon fusion*, *Phys. Rev.* **D 34** (1986) 155 [inSPIRE].

[3] S.L. Glashow, J. Iliopoulos and L. Maiani, *Weak interactions with lepton-hadron symmetry*, *Phys. Rev.* **D 2** (1970) 1285 [inSPIRE].

[4] Particle Data Group collaboration, K.A. Olive et al., *Review of particle physics*, *Chin. Phys.* **C 38** (2014) 090001 [inSPIRE].

[5] G. Eilam, J.L. Hewett and A. Soni, *Rare decays of the top quark in the standard and two Higgs doublet models*, *Phys. Rev.* **D 44** (1991) 1473 [*Erratum ibid.* **D 59** (1999) 039901] [inSPIRE].

[6] D. Atwood, L. Reina and A. Soni, *Probing flavor changing top-charm-scalar interactions in e^+e^- collisions*, *Phys. Rev.* **D 53** (1996) 1199 [`hep-ph/9506243`] [inSPIRE].

[7] J.M. Yang, B.-L. Young and X. Zhang, *Flavor changing top quark decays in R-parity violating SUSY*, *Phys. Rev.* **D 58** (1998) 055001 [`hep-ph/9705341`] [inSPIRE].

[8] Y. Grossman, *Phenomenology of models with more than two Higgs doublets*, *Nucl. Phys.* **B 426** (1994) 355 [`hep-ph/9401311`] [inSPIRE].

[9] A. Pich and P. Tuzon, *Yukawa alignment in the two-Higgs-doublet model*, *Phys. Rev.* **D 80** (2009) 091702 [`arXiv:0908.1554`] [inSPIRE].

[10] V. Keus, S.F. King and S. Moretti, *Three-Higgs-doublet models: symmetries, potentials and Higgs boson masses*, *JHEP* **01** (2014) 052 [`arXiv:1310.8253`] [inSPIRE].

[11] J.L. Diaz-Cruz, R. Martinez, M.A. Perez and A. Rosado, *Flavor changing radiative decay of the t quark*, *Phys. Rev.* **D 41** (1990) 891 [inSPIRE].

[12] A. Arhrib and W.-S. Hou, *Flavor changing neutral currents involving heavy quarks with four generations*, *JHEP* **07** (2006) 009 [`hep-ph/0602035`] [inSPIRE].

[13] G.C. Branco and M.N. Rebelo, *New physics in the flavour sector in the presence of flavour changing neutral currents*, in *Proceedings of the Corfu Summer Institute*, Greece (2012), pg. 024 [`PoS(Corfu2012)024`] [`arXiv:1308.4639`] [inSPIRE].

[14] H. Georgi, L. Kaplan, D. Morin and A. Schenk, *Effects of top compositeness*, *Phys. Rev.* **D 51** (1995) 3888 [`hep-ph/9410307`] [inSPIRE].

[15] G.F. Giudice, C. Grojean, A. Pomarol and R. Rattazzi, *The strongly-interacting light Higgs*, *JHEP* **06** (2007) 045 [`hep-ph/0703164`] [inSPIRE].

[16] M. König, M. Neubert and D.M. Straub, *Dipole operator constraints on composite Higgs models*, *Eur. Phys. J.* **C 74** (2014) 2945 [`arXiv:1403.2756`] [inSPIRE].

[17] K. Agashe, A. Azatov, Y. Cui, L. Randall and M. Son, *Warped dipole completed, with a tower of Higgs bosons*, *JHEP* **06** (2015) 196 [`arXiv:1412.6468`] [inSPIRE].

[18] R. Contino, Y. Nomura and A. Pomarol, *Higgs as a holographic pseudo-Goldstone boson*, *Nucl. Phys.* **B 671** (2003) 148 [`hep-ph/0306259`] [inSPIRE].

[19] J.A. Aguilar-Saavedra, *A minimal set of top anomalous couplings*, *Nucl. Phys.* **B 812** (2009) 181 [`arXiv:0811.3842`] [inSPIRE].

[20] S. Willenbrock and C. Zhang, *Effective field theory beyond the Standard Model*, *Ann. Rev. Nucl. Part. Sci.* **64** (2014) 83 [`arXiv:1401.0470`] [ɪɴSPIRE].

[21] CDF collaboration, T. Aaltonen et al., *Search for top-quark production via flavor-changing neutral currents in W + 1 jet events at CDF*, *Phys. Rev. Lett.* **102** (2009) 151801 [`arXiv:0812.3400`] [ɪɴSPIRE].

[22] D0 collaboration, V.M. Abazov et al., *Search for flavor changing neutral currents via quark-gluon couplings in single top quark production using* $2.3\,\mathrm{fb}^{-1}$ *of* $p\bar{p}$ *collisions*, *Phys. Lett.* **B 693** (2010) 81 [`arXiv:1006.3575`] [ɪɴSPIRE].

[23] ATLAS collaboration, *Search for single top-quark production via flavour-changing neutral currents at* $8\,TeV$ *with the ATLAS detector*, *Eur. Phys. J.* **C 76** (2016) 55 [`arXiv:1509.00294`] [ɪɴSPIRE].

[24] CMS collaboration, *Measurement of the t-channel single-top-quark production cross section and of the* $|V_{\mathrm{tb}}|$ *CKM matrix element in pp collisions at* $\sqrt{s} = 8\,TeV$, *JHEP* **06** (2014) 090 [`arXiv:1403.7366`] [ɪɴSPIRE].

[25] CMS collaboration, *Measurement of top quark polarisation in t-channel single top quark production*, *JHEP* **04** (2016) 073 [`arXiv:1511.02138`] [ɪɴSPIRE].

[26] ATLAS collaboration, *Comprehensive measurements of t-channel single top-quark production cross sections at* $\sqrt{s} = 7\,TeV$ *with the ATLAS detector*, *Phys. Rev.* **D 90** (2014) 112006 [`arXiv:1406.7844`] [ɪɴSPIRE].

[27] CompHEP collaboration, E. Boos et al., *CompHEP 4.4: automatic computations from Lagrangians to events*, *Nucl. Instrum. Meth.* **A 534** (2004) 250 [`hep-ph/0403113`] [ɪɴSPIRE].

[28] R.M. Neal, *Bayesian learning for neural networks*, technical report, Dept. of Statistics and Dept. of Computer Science, University of Toronto, Toronto Canada (1994) [ISBN:0-387-94724-8].

[29] P.C. Bhat and H.B. Prosper, *Bayesian neural networks*, in *Statistical Problems in Particle Physics, Astrophysics and Cosmology (PHYSTAT05)*, Oxford U.K. (2005), pg. 151 [*Conf. Proc.* **C 050912** (2005) 151] [ɪɴSPIRE].

[30] R.M. Neal, *Software for flexible Bayesian modeling and Markov chain sampling*, technical report 2004-11-10, Dept. of Statistics and Dept. of Computer Science, University of Toronto, Toronto Canada (2004).

[31] CMS collaboration, *The CMS experiment at the CERN LHC*, 2008 *JINST* **3** S08004 [ɪɴSPIRE].

[32] CMS collaboration, *Particle-flow event reconstruction in CMS and performance for jets, taus and MET*, CMS-PAS-PFT-09-001, CERN, Geneva Switzerland (2009).

[33] CMS collaboration, *Commissioning of the particle-flow event reconstruction with the first LHC collisions recorded in the CMS detector*, CMS-PAS-PFT-10-001, CERN, Geneva Switzerland (2010).

[34] M. Cacciari, G.P. Salam and G. Soyez, *The anti-k_t jet clustering algorithm*, *JHEP* **04** (2008) 063 [`arXiv:0802.1189`] [ɪɴSPIRE].

[35] M. Cacciari, G.P. Salam and G. Soyez, *FastJet user manual*, *Eur. Phys. J.* **C 72** (2012) 1896 [`arXiv:1111.6097`] [ɪɴSPIRE].

[36] E.E. Boos, V.E. Bunichev, L.V. Dudko, V.I. Savrin and A.V. Sherstnev, *Method for simulating electroweak top-quark production events in the NLO approximation: singleTop event generator*, *Phys. Atom. Nucl.* **69** (2006) 1317 [*Yad. Fiz.* **69** (2006) 1352] [ɪɴSPIRE].

[37] N. Kidonakis, *Next-to-next-to-leading-order collinear and soft gluon corrections for t-channel single top quark production*, *Phys. Rev.* **D 83** (2011) 091503 [arXiv:1103.2792] [ɪɴSPIRE].

[38] M. Aliev, H. Lacker, U. Langenfeld, S. Moch, P. Uwer and M. Wiedermann, *HATHOR: HAdronic Top and Heavy quarks crOss section calculatoR*, *Comput. Phys. Commun.* **182** (2011) 1034 [arXiv:1007.1327] [ɪɴSPIRE].

[39] P. Kant et al., *HatHor for single top-quark production: updated predictions and uncertainty estimates for single top-quark production in hadronic collisions*, *Comput. Phys. Commun.* **191** (2015) 74 [arXiv:1406.4403] [ɪɴSPIRE].

[40] S. Alioli, P. Nason, C. Oleari and E. Re, *A general framework for implementing NLO calculations in shower Monte Carlo programs: the POWHEG BOX*, *JHEP* **06** (2010) 043 [arXiv:1002.2581] [ɪɴSPIRE].

[41] J. Alwall, M. Herquet, F. Maltoni, O. Mattelaer and T. Stelzer, *MadGraph 5: going beyond*, *JHEP* **06** (2011) 128 [arXiv:1106.0522] [ɪɴSPIRE].

[42] M. Czakon, P. Fiedler and A. Mitov, *Total top-quark pair-production cross section at hadron colliders through $O(\alpha_S^4)$*, *Phys. Rev. Lett.* **110** (2013) 252004 [arXiv:1303.6254] [ɪɴSPIRE].

[43] M. Czakon and A. Mitov, *Top++: a program for the calculation of the top-pair cross-section at hadron colliders*, *Comput. Phys. Commun.* **185** (2014) 2930 [arXiv:1112.5675] [ɪɴSPIRE].

[44] R. Gavin, Y. Li, F. Petriello and S. Quackenbush, *FEWZ 2.0: a code for hadronic Z production at next-to-next-to-leading order*, *Comput. Phys. Commun.* **182** (2011) 2388 [arXiv:1011.3540] [ɪɴSPIRE].

[45] J.M. Campbell and R.K. Ellis, *MCFM for the Tevatron and the LHC*, *Nucl. Phys. Proc. Suppl.* **B 205-206** (2010) 10 [arXiv:1007.3492] [ɪɴSPIRE].

[46] T. Sjöstrand, S. Mrenna and P.Z. Skands, *PYTHIA 6.4 physics and manual*, *JHEP* **05** (2006) 026 [hep-ph/0603175] [ɪɴSPIRE].

[47] N. Kidonakis, *Top quark production*, arXiv:1311.0283 [ɪɴSPIRE].

[48] S. Alekhin et al., *The PDF4LHC working group interim report*, arXiv:1101.0536 [ɪɴSPIRE].

[49] J. Gao et al., *CT10 next-to-next-to-leading order global analysis of QCD*, *Phys. Rev.* **D 89** (2014) 033009 [arXiv:1302.6246] [ɪɴSPIRE].

[50] CMS collaboration, *Study of the underlying event at forward rapidity in pp collisions at $\sqrt{s} = 0.9$, 2.76 and 7 TeV*, *JHEP* **04** (2013) 072 [arXiv:1302.2394] [ɪɴSPIRE].

[51] CMS collaboration, *Event generator tunes obtained from underlying event and multiparton scattering measurements*, *Eur. Phys. J.* **C 76** (2016) 155 [arXiv:1512.00815] [ɪɴSPIRE].

[52] CMS collaboration, *Performance of CMS muon reconstruction in pp collision events at $\sqrt{s} = 7$ TeV*, 2012 *JINST* **7** P10002 [arXiv:1206.4071] [ɪɴSPIRE].

[53] CMS collaboration, *Single muon efficiencies in 2012 data*, CMS-DP-2013-009, CERN, Geneva Switzerland (2013).

[54] CMS collaboration, *Identification of b-quark jets with the CMS experiment*, 2013 *JINST* **8** P04013 [arXiv:1211.4462] [ɪɴSPIRE].

[55] G. Mahlon and S.J. Parke, *Improved spin basis for angular correlation studies in single top quark production at the Tevatron*, *Phys. Rev.* **D 55** (1997) 7249 [hep-ph/9611367] [INSPIRE].

[56] J.A. Aguilar-Saavedra and R.V. Herrero-Hahn, *Model-independent measurement of the top quark polarisation*, *Phys. Lett.* **B 718** (2013) 983 [arXiv:1208.6006] [INSPIRE].

[57] V.D. Barger and R.J.N. Phillips, *Collider physics*, *Front. Phys.* **71**, Addison-Wesley, Redwood City U.S.A. (1987).

[58] CMS collaboration, *Measurement of the t-channel single top quark production cross section in pp collisions at $\sqrt{s} = 7\,TeV$*, *Phys. Rev. Lett.* **107** (2011) 091802 [arXiv:1106.3052] [INSPIRE].

[59] CMS collaboration, *Measurement of the single-top-quark t-channel cross section in pp collisions at $\sqrt{s} = 7\,TeV$*, *JHEP* **12** (2012) 035 [arXiv:1209.4533] [INSPIRE].

[60] CMS collaboration, *Determination of jet energy calibration and transverse momentum resolution in CMS*, 2011 *JINST* **6** P11002 [arXiv:1107.4277] [INSPIRE].

[61] CMS collaboration, *Jet energy resolution in CMS at $\sqrt{s} = 7\,TeV$*, CMS-PAS-JME-10-014, CERN, Geneva Switzerland (2011).

[62] CMS collaboration, *Absolute calibration of the luminosity measurement at CMS: Winter 2012 update*, CMS-PAS-SMP-12-008, CERN, Geneva Switzerland (2012).

[63] CMS collaboration, *CMS luminosity based on pixel cluster counting: Summer 2013 update*, CMS-PAS-LUM-13-001, CERN, Geneva Switzerland (2013).

[64] CMS collaboration, *Measurement of the inelastic proton-proton cross section at $\sqrt{s} = 7\,TeV$*, *Phys. Lett.* **B 722** (2013) 5 [arXiv:1210.6718] [INSPIRE].

[65] J. Alwall, S. de Visscher and F. Maltoni, *QCD radiation in the production of heavy colored particles at the LHC*, *JHEP* **02** (2009) 017 [arXiv:0810.5350] [INSPIRE].

[66] CMS collaboration, *Measurement of differential top-quark pair production cross sections in pp colisions at $\sqrt{s} = 7\,TeV$*, *Eur. Phys. J.* **C 73** (2013) 2339 [arXiv:1211.2220] [INSPIRE].

[67] CMS collaboration, *Measurement of the differential cross section for top quark pair production in pp collisions at $\sqrt{s} = 8\,TeV$*, *Eur. Phys. J.* **C 75** (2015) 542 [arXiv:1505.04480] [INSPIRE].

[68] R.J. Barlow and C. Beeston, *Fitting using finite Monte Carlo samples*, *Comput. Phys. Commun.* **77** (1993) 219 [INSPIRE].

[69] W. Buchmüller and D. Wyler, *Effective Lagrangian analysis of new interactions and flavor conservation*, *Nucl. Phys.* **B 268** (1986) 621 [INSPIRE].

[70] G.L. Kane, G.A. Ladinsky and C.P. Yuan, *Using the top quark for testing Standard Model polarization and CP predictions*, *Phys. Rev.* **D 45** (1992) 124 [INSPIRE].

[71] D0 collaboration, V.M. Abazov et al., *Search for anomalous Wtb couplings in single top quark production*, *Phys. Rev. Lett.* **101** (2008) 221801 [arXiv:0807.1692] [INSPIRE].

[72] D0 collaboration, V.M. Abazov et al., *Search for anomalous Wtb couplings in single top quark production in $p\bar{p}$ collisions at $\sqrt{s} = 1.96\,TeV$*, *Phys. Lett.* **B 708** (2012) 21 [arXiv:1110.4592] [INSPIRE].

[73] E. Boos, V. Bunichev, L. Dudko and M. Perfilov, *Modeling of anomalous Wtb interactions using subsidiary fields*, *Int. J. Mod. Phys.* **A 32** (2017) 1750008 [arXiv:1607.00505] [INSPIRE].

[74] ATLAS collaboration, *Measurement of the W boson polarization in top quark decays with the ATLAS detector*, *JHEP* **06** (2012) 088 [`arXiv:1205.2484`] [ɪɴSPIRE].

[75] CMS collaboration, *Measurement of the W boson helicity in top-quark decays from $t\bar{t}$ production in lepton+jets events in pp collisions at $\sqrt{s} = 7\,TeV$*, *JHEP* **10** (2013) 167 [`arXiv:1308.3879`] [ɪɴSPIRE].

[76] CMS collaboration, *Measurement of the W boson helicity in events with a single reconstructed top quark in pp collisions at $\sqrt{s} = 8\,TeV$*, *JHEP* **01** (2015) 053 [`arXiv:1410.1154`] [ɪɴSPIRE].

[77] J.J. Liu, C.S. Li, L.L. Yang and L.G. Jin, *Next-to-leading order QCD corrections to the direct top quark production via model-independent FCNC couplings at hadron colliders*, *Phys. Rev.* **D 72** (2005) 074018 [`hep-ph/0508016`] [ɪɴSPIRE].

[78] J.J. Zhang et al., *Next-to-leading order QCD corrections to the top quark decay via model-independent FCNC couplings*, *Phys. Rev. Lett.* **102** (2009) 072001 [`arXiv:0810.3889`] [ɪɴSPIRE].

The CMS collaboration

Yerevan Physics Institute, Yerevan, Armenia

V. Khachatryan, A.M. Sirunyan, A. Tumasyan

Institut für Hochenergiephysik, Wien, Austria

W. Adam, E. Asilar, T. Bergauer, J. Brandstetter, E. Brondolin, M. Dragicevic, J. Erö, M. Flechl, M. Friedl, R. Frühwirth[1], V.M. Ghete, C. Hartl, N. Hörmann, J. Hrubec, M. Jeitler[1], A. König, I. Krätschmer, D. Liko, T. Matsushita, I. Mikulec, D. Rabady, N. Rad, B. Rahbaran, H. Rohringer, J. Schieck[1], J. Strauss, W. Treberer-Treberspurg, W. Waltenberger, C.-E. Wulz[1]

National Centre for Particle and High Energy Physics, Minsk, Belarus

V. Mossolov, N. Shumeiko, J. Suarez Gonzalez

Universiteit Antwerpen, Antwerpen, Belgium

S. Alderweireldt, E.A. De Wolf, X. Janssen, J. Lauwers, M. Van De Klundert, H. Van Haevermaet, P. Van Mechelen, N. Van Remortel, A. Van Spilbeeck

Vrije Universiteit Brussel, Brussel, Belgium

S. Abu Zeid, F. Blekman, J. D'Hondt, N. Daci, I. De Bruyn, K. Deroover, N. Heracleous, S. Lowette, S. Moortgat, L. Moreels, A. Olbrechts, Q. Python, S. Tavernier, W. Van Doninck, P. Van Mulders, I. Van Parijs

Université Libre de Bruxelles, Bruxelles, Belgium

H. Brun, C. Caillol, B. Clerbaux, G. De Lentdecker, H. Delannoy, G. Fasanella, L. Favart, R. Goldouzian, A. Grebenyuk, G. Karapostoli, T. Lenzi, A. Léonard, J. Luetic, T. Maerschalk, A. Marinov, A. Randle-conde, T. Seva, C. Vander Velde, P. Vanlaer, R. Yonamine, F. Zenoni, F. Zhang[2]

Ghent University, Ghent, Belgium

A. Cimmino, T. Cornelis, D. Dobur, A. Fagot, G. Garcia, M. Gul, D. Poyraz, S. Salva, R. Schöfbeck, M. Tytgat, W. Van Driessche, E. Yazgan, N. Zaganidis

Université Catholique de Louvain, Louvain-la-Neuve, Belgium

H. Bakhshiansohi, C. Beluffi[3], O. Bondu, S. Brochet, G. Bruno, A. Caudron, L. Ceard, S. De Visscher, C. Delaere, M. Delcourt, L. Forthomme, B. Francois, A. Giammanco, A. Jafari, P. Jez, M. Komm, V. Lemaitre, A. Magitteri, A. Mertens, M. Musich, C. Nuttens, K. Piotrzkowski, L. Quertenmont, M. Selvaggi, M. Vidal Marono, S. Wertz

Université de Mons, Mons, Belgium

N. Beliy

Centro Brasileiro de Pesquisas Fisicas, Rio de Janeiro, Brazil

W.L. Aldá Júnior, F.L. Alves, G.A. Alves, L. Brito, C. Hensel, A. Moraes, M.E. Pol, P. Rebello Teles

Universidade do Estado do Rio de Janeiro, Rio de Janeiro, Brazil

E. Belchior Batista Das Chagas, W. Carvalho, J. Chinellato[4], A. Custódio, E.M. Da Costa, G.G. Da Silveira, D. De Jesus Damiao, C. De Oliveira Martins, S. Fonseca De Souza, L.M. Huertas Guativa, H. Malbouisson, D. Matos Figueiredo, C. Mora Herrera, L. Mundim, H. Nogima, W.L. Prado Da Silva, A. Santoro, A. Sznajder, E.J. Tonelli Manganote[4], A. Vilela Pereira

Universidade Estadual Paulista [a], Universidade Federal do ABC [b], São Paulo, Brazil

S. Ahuja[a], C.A. Bernardes[b], S. Dogra[a], T.R. Fernandez Perez Tomei[a], E.M. Gregores[b], P.G. Mercadante[b], C.S. Moon[a], S.F. Novaes[a], Sandra S. Padula[a], D. Romero Abad[b], J.C. Ruiz Vargas

Institute for Nuclear Research and Nuclear Energy, Sofia, Bulgaria

A. Aleksandrov, R. Hadjiiska, P. Iaydjiev, M. Rodozov, S. Stoykova, G. Sultanov, M. Vutova

University of Sofia, Sofia, Bulgaria

A. Dimitrov, I. Glushkov, L. Litov, B. Pavlov, P. Petkov

Beihang University, Beijing, China

W. Fang[5]

Institute of High Energy Physics, Beijing, China

M. Ahmad, J.G. Bian, G.M. Chen, H.S. Chen, M. Chen, Y. Chen[6], T. Cheng, C.H. Jiang, D. Leggat, Z. Liu, F. Romeo, S.M. Shaheen, A. Spiezia, J. Tao, C. Wang, Z. Wang, H. Zhang, J. Zhao

State Key Laboratory of Nuclear Physics and Technology, Peking University, Beijing, China

Y. Ban, Q. Li, S. Liu, Y. Mao, S.J. Qian, D. Wang, Z. Xu

Universidad de Los Andes, Bogota, Colombia

C. Avila, A. Cabrera, L.F. Chaparro Sierra, C. Florez, J.P. Gomez, C.F. González Hernández, J.D. Ruiz Alvarez, J.C. Sanabria

University of Split, Faculty of Electrical Engineering, Mechanical Engineering and Naval Architecture, Split, Croatia

N. Godinovic, D. Lelas, I. Puljak, P.M. Ribeiro Cipriano

University of Split, Faculty of Science, Split, Croatia

Z. Antunovic, M. Kovac

Institute Rudjer Boskovic, Zagreb, Croatia

V. Brigljevic, D. Ferencek, K. Kadija, S. Micanovic, L. Sudic

University of Cyprus, Nicosia, Cyprus

A. Attikis, G. Mavromanolakis, J. Mousa, C. Nicolaou, F. Ptochos, P.A. Razis, H. Rykaczewski

Charles University, Prague, Czech Republic

M. Finger[7], M. Finger Jr.[7]

Universidad San Francisco de Quito, Quito, Ecuador

E. Carrera Jarrin

Academy of Scientific Research and Technology of the Arab Republic of Egypt, Egyptian Network of High Energy Physics, Cairo, Egypt

S. Elgammal[8], A. Mohamed[9], Y. Mohammed[10], E. Salama[8,11]

National Institute of Chemical Physics and Biophysics, Tallinn, Estonia

B. Calpas, M. Kadastik, M. Murumaa, L. Perrini, M. Raidal, A. Tiko, C. Veelken

Department of Physics, University of Helsinki, Helsinki, Finland

P. Eerola, J. Pekkanen, M. Voutilainen

Helsinki Institute of Physics, Helsinki, Finland

J. Härkönen, V. Karimäki, R. Kinnunen, T. Lampén, K. Lassila-Perini, S. Lehti, T. Lindén, P. Luukka, T. Peltola, J. Tuominiemi, E. Tuovinen, L. Wendland

Lappeenranta University of Technology, Lappeenranta, Finland

J. Talvitie, T. Tuuva

IRFU, CEA, Université Paris-Saclay, Gif-sur-Yvette, France

M. Besancon, F. Couderc, M. Dejardin, D. Denegri, B. Fabbro, J.L. Faure, C. Favaro, F. Ferri, S. Ganjour, S. Ghosh, A. Givernaud, P. Gras, G. Hamel de Monchenault, P. Jarry, I. Kucher, E. Locci, M. Machet, J. Malcles, J. Rander, A. Rosowsky, M. Titov, A. Zghiche

Laboratoire Leprince-Ringuet, Ecole Polytechnique, IN2P3-CNRS, Palaiseau, France

A. Abdulsalam, I. Antropov, S. Baffioni, F. Beaudette, P. Busson, L. Cadamuro, E. Chapon, C. Charlot, O. Davignon, R. Granier de Cassagnac, M. Jo, S. Lisniak, P. Miné, I.N. Naranjo, M. Nguyen, C. Ochando, G. Ortona, P. Paganini, P. Pigard, S. Regnard, R. Salerno, Y. Sirois, T. Strebler, Y. Yilmaz, A. Zabi

Institut Pluridisciplinaire Hubert Curien, Université de Strasbourg, Université de Haute Alsace Mulhouse, CNRS/IN2P3, Strasbourg, France

J.-L. Agram[12], J. Andrea, A. Aubin, D. Bloch, J.-M. Brom, M. Buttignol, E.C. Chabert, N. Chanon, C. Collard, E. Conte[12], X. Coubez, J.-C. Fontaine[12], D. Gelé, U. Goerlach, A.-C. Le Bihan, J.A. Merlin[13], K. Skovpen, P. Van Hove

Centre de Calcul de l'Institut National de Physique Nucleaire et de Physique des Particules, CNRS/IN2P3, Villeurbanne, France

S. Gadrat

Université de Lyon, Université Claude Bernard Lyon 1, CNRS-IN2P3, Institut de Physique Nucléaire de Lyon, Villeurbanne, France

S. Beauceron, C. Bernet, G. Boudoul, E. Bouvier, C.A. Carrillo Montoya, R. Chierici, D. Contardo, B. Courbon, P. Depasse, H. El Mamouni, J. Fan, J. Fay, S. Gascon,

M. Gouzevitch, G. Grenier, B. Ille, F. Lagarde, I.B. Laktineh, M. Lethuillier, L. Mirabito, A.L. Pequegnot, S. Perries, A. Popov[14], D. Sabes, V. Sordini, M. Vander Donckt, P. Verdier, S. Viret

Georgian Technical University, Tbilisi, Georgia

T. Toriashvili[15]

Tbilisi State University, Tbilisi, Georgia

Z. Tsamalaidze[7]

RWTH Aachen University, I. Physikalisches Institut, Aachen, Germany

C. Autermann, S. Beranek, L. Feld, A. Heister, M.K. Kiesel, K. Klein, M. Lipinski, A. Ostapchuk, M. Preuten, F. Raupach, S. Schael, C. Schomakers, J.F. Schulte, J. Schulz, T. Verlage, H. Weber, V. Zhukov[14]

RWTH Aachen University, III. Physikalisches Institut A, Aachen, Germany

M. Brodski, E. Dietz-Laursonn, D. Duchardt, M. Endres, M. Erdmann, S. Erdweg, T. Esch, R. Fischer, A. Güth, T. Hebbeker, C. Heidemann, K. Hoepfner, S. Knutzen, M. Merschmeyer, A. Meyer, P. Millet, S. Mukherjee, M. Olschewski, K. Padeken, P. Papacz, T. Pook, M. Radziej, H. Reithler, M. Rieger, F. Scheuch, L. Sonnenschein, D. Teyssier, S. Thüer

RWTH Aachen University, III. Physikalisches Institut B, Aachen, Germany

V. Cherepanov, Y. Erdogan, G. Flügge, W. Haj Ahmad, F. Hoehle, B. Kargoll, T. Kress, A. Künsken, J. Lingemann, A. Nehrkorn, A. Nowack, I.M. Nugent, C. Pistone, O. Pooth, A. Stahl[13]

Deutsches Elektronen-Synchrotron, Hamburg, Germany

M. Aldaya Martin, C. Asawatangtrakuldee, I. Asin, K. Beernaert, O. Behnke, U. Behrens, A.A. Bin Anuar, K. Borras[16], A. Campbell, P. Connor, C. Contreras-Campana, F. Costanza, C. Diez Pardos, G. Dolinska, G. Eckerlin, D. Eckstein, E. Gallo[17], J. Garay Garcia, A. Geiser, A. Gizhko, J.M. Grados Luyando, P. Gunnellini, A. Harb, J. Hauk, M. Hempel[18], H. Jung, A. Kalogeropoulos, O. Karacheban[18], M. Kasemann, J. Keaveney, J. Kieseler, C. Kleinwort, I. Korol, W. Lange, A. Lelek, J. Leonard, K. Lipka, A. Lobanov, W. Lohmann[18], R. Mankel, I.-A. Melzer-Pellmann, A.B. Meyer, G. Mittag, J. Mnich, A. Mussgiller, E. Ntomari, D. Pitzl, R. Placakyte, A. Raspereza, B. Roland, M.Ö. Sahin, P. Saxena, T. Schoerner-Sadenius, C. Seitz, S. Spannagel, N. Stefaniuk, K.D. Trippkewitz, G.P. Van Onsem, R. Walsh, C. Wissing

University of Hamburg, Hamburg, Germany

V. Blobel, M. Centis Vignali, A.R. Draeger, T. Dreyer, E. Garutti, K. Goebel, D. Gonzalez, J. Haller, M. Hoffmann, A. Junkes, R. Klanner, R. Kogler, N. Kovalchuk, T. Lapsien, T. Lenz, I. Marchesini, D. Marconi, M. Meyer, M. Niedziela, D. Nowatschin, J. Ott, F. Pantaleo[13], T. Peiffer, A. Perieanu, J. Poehlsen, C. Sander, C. Scharf, P. Schleper, A. Schmidt, S. Schumann, J. Schwandt, H. Stadie, G. Steinbrück, F.M. Stober, M. Stöver, H. Tholen, D. Troendle, E. Usai, L. Vanelderen, A. Vanhoefer, B. Vormwald

Institut für Experimentelle Kernphysik, Karlsruhe, Germany

C. Barth, C. Baus, J. Berger, E. Butz, T. Chwalek, F. Colombo, W. De Boer, A. Dierlamm, S. Fink, R. Friese, M. Giffels, A. Gilbert, D. Haitz, F. Hartmann[13], S.M. Heindl, U. Husemann, I. Katkov[14], P. Lobelle Pardo, B. Maier, H. Mildner, M.U. Mozer, T. Müller, Th. Müller, M. Plagge, G. Quast, K. Rabbertz, S. Röcker, F. Roscher, M. Schröder, G. Sieber, H.J. Simonis, R. Ulrich, J. Wagner-Kuhr, S. Wayand, M. Weber, T. Weiler, S. Williamson, C. Wöhrmann, R. Wolf

Institute of Nuclear and Particle Physics (INPP), NCSR Demokritos, Aghia Paraskevi, Greece

G. Anagnostou, G. Daskalakis, T. Geralis, V.A. Giakoumopoulou, A. Kyriakis, D. Loukas, I. Topsis-Giotis

National and Kapodistrian University of Athens, Athens, Greece

A. Agapitos, S. Kesisoglou, A. Panagiotou, N. Saoulidou, E. Tziaferi

University of Ioánnina, Ioánnina, Greece

I. Evangelou, G. Flouris, C. Foudas, P. Kokkas, N. Loukas, N. Manthos, I. Papadopoulos, E. Paradas

MTA-ELTE Lendület CMS Particle and Nuclear Physics Group, Eötvös Loránd University, Budapest, Hungary

N. Filipovic

Wigner Research Centre for Physics, Budapest, Hungary

G. Bencze, C. Hajdu, P. Hidas, D. Horvath[19], F. Sikler, V. Veszpremi, G. Vesztergombi[20], A.J. Zsigmond

Institute of Nuclear Research ATOMKI, Debrecen, Hungary

N. Beni, S. Czellar, J. Karancsi[21], A. Makovec, J. Molnar, Z. Szillasi

University of Debrecen, Debrecen, Hungary

M. Bartók[20], P. Raics, Z.L. Trocsanyi, B. Ujvari

National Institute of Science Education and Research, Bhubaneswar, India

S. Bahinipati, S. Choudhury[22], P. Mal, K. Mandal, A. Nayak[23], D.K. Sahoo, N. Sahoo, S.K. Swain

Panjab University, Chandigarh, India

S. Bansal, S.B. Beri, V. Bhatnagar, R. Chawla, U.Bhawandeep, A.K. Kalsi, A. Kaur, M. Kaur, R. Kumar, A. Mehta, M. Mittal, J.B. Singh, G. Walia

University of Delhi, Delhi, India

Ashok Kumar, A. Bhardwaj, B.C. Choudhary, R.B. Garg, S. Keshri, A. Kumar, S. Malhotra, M. Naimuddin, N. Nishu, K. Ranjan, R. Sharma, V. Sharma

Saha Institute of Nuclear Physics, Kolkata, India

R. Bhattacharya, S. Bhattacharya, K. Chatterjee, S. Dey, S. Dutt, S. Dutta, S. Ghosh, N. Majumdar, A. Modak, K. Mondal, S. Mukhopadhyay, S. Nandan, A. Purohit, A. Roy, D. Roy, S. Roy Chowdhury, S. Sarkar, M. Sharan, S. Thakur

Indian Institute of Technology Madras, Madras, India

P.K. Behera

Bhabha Atomic Research Centre, Mumbai, India

R. Chudasama, D. Dutta, V. Jha, V. Kumar, A.K. Mohanty[13], P.K. Netrakanti, L.M. Pant, P. Shukla, A. Topkar

Tata Institute of Fundamental Research-A, Mumbai, India

T. Aziz, S. Dugad, G. Kole, B. Mahakud, S. Mitra, G.B. Mohanty, N. Sur, B. Sutar

Tata Institute of Fundamental Research-B, Mumbai, India

S. Banerjee, S. Bhowmik[24], R.K. Dewanjee, S. Ganguly, M. Guchait, Sa. Jain, S. Kumar, M. Maity[24], G. Majumder, K. Mazumdar, B. Parida, T. Sarkar[24], N. Wickramage[25]

Indian Institute of Science Education and Research (IISER), Pune, India

S. Chauhan, S. Dube, A. Kapoor, K. Kothekar, A. Rane, S. Sharma

Institute for Research in Fundamental Sciences (IPM), Tehran, Iran

H. Behnamian, S. Chenarani[26], E. Eskandari Tadavani, S.M. Etesami[26], A. Fahim[27], M. Khakzad, M. Mohammadi Najafabadi, M. Naseri, S. Paktinat Mehdiabadi, F. Rezaei Hosseinabadi, B. Safarzadeh[28], M. Zeinali

University College Dublin, Dublin, Ireland

M. Felcini, M. Grunewald

INFN Sezione di Bari ^{a}, Università di Bari ^{b}, Politecnico di Bari ^{c}, Bari, Italy

M. Abbrescia^{a,b}, C. Calabria^{a,b}, C. Caputo^{a,b}, A. Colaleo^a, D. Creanza^{a,c}, L. Cristella^{a,b}, N. De Filippis^{a,c}, M. De Palma^{a,b}, L. Fiore^a, G. Iaselli^{a,c}, G. Maggi^{a,c}, M. Maggi^a, G. Miniello^{a,b}, S. My^{a,b}, S. Nuzzo^{a,b}, A. Pompili^{a,b}, G. Pugliese^{a,c}, R. Radogna^{a,b}, A. Ranieri^a, G. Selvaggi^{a,b}, L. Silvestris^{a,13}, R. Venditti^{a,b}, P. Verwilligen^a

INFN Sezione di Bologna ^{a}, Università di Bologna ^{b}, Bologna, Italy

G. Abbiendi^a, C. Battilana, D. Bonacorsi^{a,b}, S. Braibant-Giacomelli^{a,b}, L. Brigliadori^{a,b}, R. Campanini^{a,b}, P. Capiluppi^{a,b}, A. Castro^{a,b}, F.R. Cavallo^a, S.S. Chhibra^{a,b}, G. Codispoti^{a,b}, M. Cuffiani^{a,b}, G.M. Dallavalle^a, F. Fabbri^a, A. Fanfani^{a,b}, D. Fasanella^{a,b}, P. Giacomelli^a, C. Grandi^a, L. Guiducci^{a,b}, S. Marcellini^a, G. Masetti^a, A. Montanari^a, F.L. Navarria^{a,b}, A. Perrotta^a, A.M. Rossi^{a,b}, T. Rovelli^{a,b}, G.P. Siroli^{a,b}, N. Tosi^{a,b,13}

INFN Sezione di Catania ^{a}, Università di Catania ^{b}, Catania, Italy

S. Albergo^{a,b}, M. Chiorboli^{a,b}, S. Costa^{a,b}, A. Di Mattia^a, F. Giordano^{a,b}, R. Potenza^{a,b}, A. Tricomi^{a,b}, C. Tuve^{a,b}

INFN Sezione di Firenze [a], **Università di Firenze** [b], **Firenze, Italy**

G. Barbagli[a], V. Ciulli[a,b], C. Civinini[a], R. D'Alessandro[a,b], E. Focardi[a,b], V. Gori[a,b], P. Lenzi[a,b], M. Meschini[a], S. Paoletti[a], G. Sguazzoni[a], L. Viliani[a,b,13]

INFN Laboratori Nazionali di Frascati, Frascati, Italy

L. Benussi, S. Bianco, F. Fabbri, D. Piccolo, F. Primavera[13]

INFN Sezione di Genova [a], **Università di Genova** [b], **Genova, Italy**

V. Calvelli[a,b], F. Ferro[a], M. Lo Vetere[a,b], M.R. Monge[a,b], E. Robutti[a], S. Tosi[a,b]

INFN Sezione di Milano-Bicocca [a], **Università di Milano-Bicocca** [b], **Milano, Italy**

L. Brianza, M.E. Dinardo[a,b], S. Fiorendi[a,b], S. Gennai[a], A. Ghezzi[a,b], P. Govoni[a,b], S. Malvezzi[a], R.A. Manzoni[a,b,13], B. Marzocchi[a,b], D. Menasce[a], L. Moroni[a], M. Paganoni[a,b], D. Pedrini[a], S. Pigazzini, S. Ragazzi[a,b], T. Tabarelli de Fatis[a,b]

INFN Sezione di Napoli [a], **Università di Napoli 'Federico II'** [b], **Napoli, Italy, Università della Basilicata** [c], **Potenza, Italy, Università G. Marconi** [d], **Roma, Italy**

S. Buontempo[a], N. Cavallo[a,c], G. De Nardo, S. Di Guida[a,d,13], M. Esposito[a,b], F. Fabozzi[a,c], A.O.M. Iorio[a,b], G. Lanza[a], L. Lista[a], S. Meola[a,d,13], P. Paolucci[a,13], C. Sciacca[a,b], F. Thyssen

INFN Sezione di Padova [a], **Università di Padova** [b], **Padova, Italy, Università di Trento** [c], **Trento, Italy**

P. Azzi[a,13], N. Bacchetta[a], L. Benato[a,b], D. Bisello[a,b], A. Boletti[a,b], R. Carlin[a,b], A. Carvalho Antunes De Oliveira[a,b], P. Checchia[a], M. Dall'Osso[a,b], P. De Castro Manzano[a], T. Dorigo[a], U. Dosselli[a], F. Gasparini[a,b], U. Gasparini[a,b], A. Gozzelino[a], S. Lacaprara[a], M. Margoni[a,b], A.T. Meneguzzo[a,b], J. Pazzini[a,b,13], N. Pozzobon[a,b], P. Ronchese[a,b], F. Simonetto[a,b], E. Torassa[a], M. Zanetti, P. Zotto[a,b], A. Zucchetta[a,b], G. Zumerle[a,b]

INFN Sezione di Pavia [a], **Università di Pavia** [b], **Pavia, Italy**

A. Braghieri[a], A. Magnani[a,b], P. Montagna[a,b], S.P. Ratti[a,b], V. Re[a], C. Riccardi[a,b], P. Salvini[a], I. Vai[a,b], P. Vitulo[a,b]

INFN Sezione di Perugia [a], **Università di Perugia** [b], **Perugia, Italy**

L. Alunni Solestizi[a,b], G.M. Bilei[a], D. Ciangottini[a,b], L. Fanò[a,b], P. Lariccia[a,b], R. Leonardi[a,b], G. Mantovani[a,b], M. Menichelli[a], A. Saha[a], A. Santocchia[a,b]

INFN Sezione di Pisa [a], **Università di Pisa** [b], **Scuola Normale Superiore di Pisa** [c], **Pisa, Italy**

K. Androsov[a,29], P. Azzurri[a,13], G. Bagliesi[a], J. Bernardini[a], T. Boccali[a], R. Castaldi[a], M.A. Ciocci[a,29], R. Dell'Orso[a], S. Donato[a,c], G. Fedi, A. Giassi[a], M.T. Grippo[a,29], F. Ligabue[a,c], T. Lomtadze[a], L. Martini[a,b], A. Messineo[a,b], F. Palla[a], A. Rizzi[a,b], A. Savoy-Navarro[a,30], P. Spagnolo[a], R. Tenchini[a], G. Tonelli[a,b], A. Venturi[a], P.G. Verdini[a]

INFN Sezione di Roma ^{a}**, Università di Roma** ^{b}**, Roma, Italy**

L. Barone^{a,b}, F. Cavallari^a, M. Cipriani^{a,b}, G. D'imperio^{a,b,13}, D. Del Re^{a,b,13}, M. Diemoz^a, S. Gelli^{a,b}, C. Jorda^a, E. Longo^{a,b}, F. Margaroli^{a,b}, P. Meridiani^a, G. Organtini^{a,b}, R. Paramatti^a, F. Preiato^{a,b}, S. Rahatlou^{a,b}, C. Rovelli^a, F. Santanastasio^{a,b}

INFN Sezione di Torino ^{a}**, Università di Torino** ^{b}**, Torino, Italy, Università del Piemonte Orientale** ^{c}**, Novara, Italy**

N. Amapane^{a,b}, R. Arcidiacono^{a,c,13}, S. Argiro^{a,b}, M. Arneodo^{a,c}, N. Bartosik^a, R. Bellan^{a,b}, C. Biino^a, N. Cartiglia^a, F. Cenna^{a,b}, M. Costa^{a,b}, R. Covarelli^{a,b}, A. Degano^{a,b}, N. Demaria^a, L. Finco^{a,b}, B. Kiani^{a,b}, C. Mariotti^a, S. Maselli^a, E. Migliore^{a,b}, V. Monaco^{a,b}, E. Monteil^{a,b}, M.M. Obertino^{a,b}, L. Pacher^{a,b}, N. Pastrone^a, M. Pelliccioni^a, G.L. Pinna Angioni^{a,b}, F. Ravera^{a,b}, A. Romero^{a,b}, M. Ruspa^{a,c}, R. Sacchi^{a,b}, K. Shchelina^{a,b}, V. Sola^a, A. Solano^{a,b}, A. Staiano^a, P. Traczyk^{a,b}

INFN Sezione di Trieste ^{a}**, Università di Trieste** ^{b}**, Trieste, Italy**

S. Belforte^a, M. Casarsa^a, F. Cossutti^a, G. Della Ricca^{a,b}, C. La Licata^{a,b}, A. Schizzi^{a,b}, A. Zanetti^a

Kyungpook National University, Daegu, Korea

D.H. Kim, G.N. Kim, M.S. Kim, S. Lee, S.W. Lee, Y.D. Oh, S. Sekmen, D.C. Son, Y.C. Yang

Chonbuk National University, Jeonju, Korea

A. Lee

Hanyang University, Seoul, Korea

J.A. Brochero Cifuentes, T.J. Kim

Korea University, Seoul, Korea

S. Cho, S. Choi, Y. Go, D. Gyun, S. Ha, B. Hong, Y. Jo, Y. Kim, B. Lee, K. Lee, K.S. Lee, S. Lee, J. Lim, S.K. Park, Y. Roh

Seoul National University, Seoul, Korea

J. Almond, J. Kim, S.B. Oh, S.h. Seo, U.K. Yang, H.D. Yoo, G.B. Yu

University of Seoul, Seoul, Korea

M. Choi, H. Kim, H. Kim, J.H. Kim, J.S.H. Lee, I.C. Park, G. Ryu, M.S. Ryu

Sungkyunkwan University, Suwon, Korea

Y. Choi, J. Goh, C. Hwang, J. Lee, I. Yu

Vilnius University, Vilnius, Lithuania

V. Dudenas, A. Juodagalvis, J. Vaitkus

National Centre for Particle Physics, Universiti Malaya, Kuala Lumpur, Malaysia

I. Ahmed, Z.A. Ibrahim, J.R. Komaragiri, M.A.B. Md Ali[31], F. Mohamad Idris[32], W.A.T. Wan Abdullah, M.N. Yusli, Z. Zolkapli

Centro de Investigacion y de Estudios Avanzados del IPN, Mexico City, Mexico

H. Castilla-Valdez, E. De La Cruz-Burelo, I. Heredia-De La Cruz[33], A. Hernandez-Almada, R. Lopez-Fernandez, J. Mejia Guisao, A. Sanchez-Hernandez

Universidad Iberoamericana, Mexico City, Mexico

S. Carrillo Moreno, C. Oropeza Barrera, F. Vazquez Valencia

Benemerita Universidad Autonoma de Puebla, Puebla, Mexico

S. Carpinteyro, I. Pedraza, H.A. Salazar Ibarguen, C. Uribe Estrada

Universidad Autónoma de San Luis Potosí, San Luis Potosí, Mexico

A. Morelos Pineda

University of Auckland, Auckland, New Zealand

D. Krofcheck

University of Canterbury, Christchurch, New Zealand

P.H. Butler

National Centre for Physics, Quaid-I-Azam University, Islamabad, Pakistan

A. Ahmad, M. Ahmad, Q. Hassan, H.R. Hoorani, W.A. Khan, M.A. Shah, M. Shoaib, M. Waqas

National Centre for Nuclear Research, Swierk, Poland

H. Bialkowska, M. Bluj, B. Boimska, T. Frueboes, M. Górski, M. Kazana, K. Nawrocki, K. Romanowska-Rybinska, M. Szleper, P. Zalewski

Institute of Experimental Physics, Faculty of Physics, University of Warsaw, Warsaw, Poland

K. Bunkowski, A. Byszuk[34], K. Doroba, A. Kalinowski, M. Konecki, J. Krolikowski, M. Misiura, M. Olszewski, M. Walczak

Laboratório de Instrumentação e Física Experimental de Partículas, Lisboa, Portugal

P. Bargassa, C. Beirão Da Cruz E Silva, A. Di Francesco, P. Faccioli, P.G. Ferreira Parracho, M. Gallinaro, J. Hollar, N. Leonardo, L. Lloret Iglesias, M.V. Nemallapudi, J. Rodrigues Antunes, J. Seixas, O. Toldaiev, D. Vadruccio, J. Varela, P. Vischia

Joint Institute for Nuclear Research, Dubna, Russia

A. Golunov, I. Golutvin, N. Gorbounov, A. Kamenev, V. Karjavin, V. Korenkov, A. Lanev, A. Malakhov, V. Matveev[35,36], V.V. Mitsyn, P. Moisenz, V. Palichik, V. Perelygin, S. Shmatov, S. Shulha, N. Skatchkov, V. Smirnov, E. Tikhonenko, A. Zarubin

Petersburg Nuclear Physics Institute, Gatchina (St. Petersburg), Russia

L. Chtchipounov, V. Golovtsov, Y. Ivanov, V. Kim[37], E. Kuznetsova[38], V. Murzin, V. Oreshkin, V. Sulimov, A. Vorobyev

Institute for Nuclear Research, Moscow, Russia

Yu. Andreev, A. Dermenev, S. Gninenko, N. Golubev, A. Karneyeu, M. Kirsanov, N. Krasnikov, A. Pashenkov, D. Tlisov, A. Toropin

Institute for Theoretical and Experimental Physics, Moscow, Russia

V. Epshteyn, V. Gavrilov, N. Lychkovskaya, V. Popov, I. Pozdnyakov, G. Safronov, A. Spiridonov, M. Toms, E. Vlasov, A. Zhokin

National Research Nuclear University 'Moscow Engineering Physics Institute' (MEPhI), Moscow, Russia

M. Chadeeva[39], M. Danilov[39], O. Markin

P.N. Lebedev Physical Institute, Moscow, Russia

V. Andreev, M. Azarkin[36], I. Dremin[36], M. Kirakosyan, A. Leonidov[36], S.V. Rusakov, A. Terkulov

Skobeltsyn Institute of Nuclear Physics, Lomonosov Moscow State University, Moscow, Russia

A. Baskakov, A. Belyaev, E. Boos, V. Bunichev, M. Dubinin[40], L. Dudko, V. Klyukhin, O. Kodolova, N. Korneeva, I. Lokhtin, I. Miagkov, S. Obraztsov, M. Perfilov, V. Savrin, P. Volkov, G. Vorotnikov

State Research Center of Russian Federation, Institute for High Energy Physics, Protvino, Russia

I. Azhgirey, I. Bayshev, S. Bitioukov, D. Elumakhov, V. Kachanov, A. Kalinin, D. Konstantinov, V. Krychkine, V. Petrov, R. Ryutin, A. Sobol, S. Troshin, N. Tyurin, A. Uzunian, A. Volkov

University of Belgrade, Faculty of Physics and Vinca Institute of Nuclear Sciences, Belgrade, Serbia

P. Adzic[41], P. Cirkovic, D. Devetak, J. Milosevic, V. Rekovic

Centro de Investigaciones Energéticas Medioambientales y Tecnológicas (CIEMAT), Madrid, Spain

J. Alcaraz Maestre, E. Calvo, M. Cerrada, M. Chamizo Llatas, N. Colino, B. De La Cruz, A. Delgado Peris, A. Escalante Del Valle, C. Fernandez Bedoya, J.P. Fernández Ramos, J. Flix, M.C. Fouz, P. Garcia-Abia, O. Gonzalez Lopez, S. Goy Lopez, J.M. Hernandez, M.I. Josa, E. Navarro De Martino, A. Pérez-Calero Yzquierdo, J. Puerta Pelayo, A. Quintario Olmeda, I. Redondo, L. Romero, M.S. Soares

Universidad Autónoma de Madrid, Madrid, Spain

J.F. de Trocóniz, M. Missiroli, D. Moran

Universidad de Oviedo, Oviedo, Spain

J. Cuevas, J. Fernandez Menendez, I. Gonzalez Caballero, J.R. González Fernández, E. Palencia Cortezon, S. Sanchez Cruz, I. Suárez Andrés, J.M. Vizan Garcia

Instituto de Física de Cantabria (IFCA), CSIC-Universidad de Cantabria, Santander, Spain

I.J. Cabrillo, A. Calderon, J.R. Castiñeiras De Saa, E. Curras, M. Fernandez, J. Garcia-Ferrero, G. Gomez, A. Lopez Virto, J. Marco, C. Martinez Rivero, F. Matorras, J. Piedra

Gomez, T. Rodrigo, A. Ruiz-Jimeno, L. Scodellaro, N. Trevisani, I. Vila, R. Vilar Cortabitarte

CERN, European Organization for Nuclear Research, Geneva, Switzerland

D. Abbaneo, E. Auffray, G. Auzinger, M. Bachtis, P. Baillon, A.H. Ball, D. Barney, P. Bloch, A. Bocci, A. Bonato, C. Botta, T. Camporesi, R. Castello, M. Cepeda, G. Cerminara, M. D'Alfonso, D. d'Enterria, A. Dabrowski, V. Daponte, A. David, M. De Gruttola, F. De Guio, A. De Roeck, E. Di Marco[42], M. Dobson, M. Dordevic, B. Dorney, T. du Pree, D. Duggan, M. Dünser, N. Dupont, A. Elliott-Peisert, S. Fartoukh, G. Franzoni, J. Fulcher, W. Funk, D. Gigi, K. Gill, M. Girone, F. Glege, D. Gulhan, S. Gundacker, M. Guthoff, J. Hammer, P. Harris, J. Hegeman, V. Innocente, P. Janot, H. Kirschenmann, V. Knünz, A. Kornmayer[13], M.J. Kortelainen, K. Kousouris, M. Krammer[1], P. Lecoq, C. Lourenço, M.T. Lucchini, L. Malgeri, M. Mannelli, A. Martelli, F. Meijers, S. Mersi, E. Meschi, F. Moortgat, S. Morovic, M. Mulders, H. Neugebauer, S. Orfanelli[43], L. Orsini, L. Pape, E. Perez, M. Peruzzi, A. Petrilli, G. Petrucciani, A. Pfeiffer, M. Pierini, A. Racz, T. Reis, G. Rolandi[44], M. Rovere, M. Ruan, H. Sakulin, J.B. Sauvan, C. Schäfer, C. Schwick, M. Seidel, A. Sharma, P. Silva, M. Simon, P. Sphicas[45], J. Steggemann, M. Stoye, Y. Takahashi, M. Tosi, D. Treille, A. Triossi, A. Tsirou, V. Veckalns[46], G.I. Veres[20], N. Wardle, H.K. Wöhri, A. Zagozdzinska[34], W.D. Zeuner

Paul Scherrer Institut, Villigen, Switzerland

W. Bertl, K. Deiters, W. Erdmann, R. Horisberger, Q. Ingram, H.C. Kaestli, D. Kotlinski, U. Langenegger, T. Rohe

Institute for Particle Physics, ETH Zurich, Zurich, Switzerland

F. Bachmair, L. Bäni, L. Bianchini, B. Casal, G. Dissertori, M. Dittmar, M. Donegà, P. Eller, C. Grab, C. Heidegger, D. Hits, J. Hoss, G. Kasieczka, P. Lecomte[†], W. Lustermann, B. Mangano, M. Marionneau, P. Martinez Ruiz del Arbol, M. Masciovecchio, M.T. Meinhard, D. Meister, F. Micheli, P. Musella, F. Nessi-Tedaldi, F. Pandolfi, J. Pata, F. Pauss, G. Perrin, L. Perrozzi, M. Quittnat, M. Rossini, M. Schönenberger, A. Starodumov[47], M. Takahashi, V.R. Tavolaro, K. Theofilatos, R. Wallny

Universität Zürich, Zurich, Switzerland

T.K. Aarrestad, C. Amsler[48], L. Caminada, M.F. Canelli, V. Chiochia, A. De Cosa, C. Galloni, A. Hinzmann, T. Hreus, B. Kilminster, C. Lange, J. Ngadiuba, D. Pinna, G. Rauco, P. Robmann, D. Salerno, Y. Yang

National Central University, Chung-Li, Taiwan

V. Candelise, T.H. Doan, Sh. Jain, R. Khurana, M. Konyushikhin, C.M. Kuo, W. Lin, Y.J. Lu, A. Pozdnyakov, S.S. Yu

National Taiwan University (NTU), Taipei, Taiwan

Arun Kumar, P. Chang, Y.H. Chang, Y.W. Chang, Y. Chao, K.F. Chen, P.H. Chen, C. Dietz, F. Fiori, W.-S. Hou, Y. Hsiung, Y.F. Liu, R.-S. Lu, M. Miñano Moya, E. Paganis, A. Psallidas, J.f. Tsai, Y.M. Tzeng

Chulalongkorn University, Faculty of Science, Department of Physics, Bangkok, Thailand

B. Asavapibhop, G. Singh, N. Srimanobhas, N. Suwonjandee

Cukurova University, Adana, Turkey

A. Adiguzel, M.N. Bakirci[49], S. Cerci[50], S. Damarseckin, Z.S. Demiroglu, C. Dozen, I. Dumanoglu, S. Girgis, G. Gokbulut, Y. Guler, E. Gurpinar, I. Hos, E.E. Kangal[51], O. Kara, A. Kayis Topaksu, U. Kiminsu, M. Oglakci, G. Onengut[52], K. Ozdemir[53], B. Tali[50], S. Turkcapar, I.S. Zorbakir, C. Zorbilmez

Middle East Technical University, Physics Department, Ankara, Turkey

B. Bilin, S. Bilmis, B. Isildak[54], G. Karapinar[55], M. Yalvac, M. Zeyrek

Bogazici University, Istanbul, Turkey

E. Gülmez, M. Kaya[56], O. Kaya[57], E.A. Yetkin[58], T. Yetkin[59]

Istanbul Technical University, Istanbul, Turkey

A. Cakir, K. Cankocak, S. Sen[60]

Institute for Scintillation Materials of National Academy of Science of Ukraine, Kharkov, Ukraine

B. Grynyov

National Scientific Center, Kharkov Institute of Physics and Technology, Kharkov, Ukraine

L. Levchuk, P. Sorokin

University of Bristol, Bristol, United Kingdom

R. Aggleton, F. Ball, L. Beck, J.J. Brooke, D. Burns, E. Clement, D. Cussans, H. Flacher, J. Goldstein, M. Grimes, G.P. Heath, H.F. Heath, J. Jacob, L. Kreczko, C. Lucas, D.M. Newbold[61], S. Paramesvaran, A. Poll, T. Sakuma, S. Seif El Nasr-storey, D. Smith, V.J. Smith

Rutherford Appleton Laboratory, Didcot, United Kingdom

K.W. Bell, A. Belyaev[62], C. Brew, R.M. Brown, L. Calligaris, D. Cieri, D.J.A. Cockerill, J.A. Coughlan, K. Harder, S. Harper, E. Olaiya, D. Petyt, C.H. Shepherd-Themistocleous, A. Thea, I.R. Tomalin, T. Williams

Imperial College, London, United Kingdom

M. Baber, R. Bainbridge, O. Buchmuller, A. Bundock, D. Burton, S. Casasso, M. Citron, D. Colling, L. Corpe, P. Dauncey, G. Davies, A. De Wit, M. Della Negra, P. Dunne, A. Elwood, D. Futyan, Y. Haddad, G. Hall, G. Iles, R. Lane, C. Laner, R. Lucas[61], L. Lyons, A.-M. Magnan, S. Malik, L. Mastrolorenzo, J. Nash, A. Nikitenko[47], J. Pela, B. Penning, M. Pesaresi, D.M. Raymond, A. Richards, A. Rose, C. Seez, A. Tapper, K. Uchida, M. Vazquez Acosta[63], T. Virdee[13], S.C. Zenz

Brunel University, Uxbridge, United Kingdom

J.E. Cole, P.R. Hobson, A. Khan, P. Kyberd, D. Leslie, I.D. Reid, P. Symonds, L. Teodorescu, M. Turner

Baylor University, Waco, U.S.A.

A. Borzou, K. Call, J. Dittmann, K. Hatakeyama, H. Liu, N. Pastika

The University of Alabama, Tuscaloosa, U.S.A.

O. Charaf, S.I. Cooper, C. Henderson, P. Rumerio

Boston University, Boston, U.S.A.

D. Arcaro, A. Avetisyan, T. Bose, D. Gastler, D. Rankin, C. Richardson, J. Rohlf, L. Sulak, D. Zou

Brown University, Providence, U.S.A.

G. Benelli, E. Berry, D. Cutts, A. Garabedian, J. Hakala, U. Heintz, J.M. Hogan, O. Jesus, E. Laird, G. Landsberg, Z. Mao, M. Narain, S. Piperov, S. Sagir, E. Spencer, R. Syarif

University of California, Davis, Davis, U.S.A.

R. Breedon, G. Breto, D. Burns, M. Calderon De La Barca Sanchez, S. Chauhan, M. Chertok, J. Conway, R. Conway, P.T. Cox, R. Erbacher, C. Flores, G. Funk, M. Gardner, W. Ko, R. Lander, C. Mclean, M. Mulhearn, D. Pellett, J. Pilot, F. Ricci-Tam, S. Shalhout, J. Smith, M. Squires, D. Stolp, M. Tripathi, S. Wilbur, R. Yohay

University of California, Los Angeles, U.S.A.

R. Cousins, P. Everaerts, A. Florent, J. Hauser, M. Ignatenko, D. Saltzberg, E. Takasugi, V. Valuev, M. Weber

University of California, Riverside, Riverside, U.S.A.

K. Burt, R. Clare, J. Ellison, J.W. Gary, G. Hanson, J. Heilman, P. Jandir, E. Kennedy, F. Lacroix, O.R. Long, M. Malberti, M. Olmedo Negrete, M.I. Paneva, A. Shrinivas, H. Wei, S. Wimpenny, B. R. Yates

University of California, San Diego, La Jolla, U.S.A.

J.G. Branson, G.B. Cerati, S. Cittolin, M. Derdzinski, R. Gerosa, A. Holzner, D. Klein, V. Krutelyov, J. Letts, I. Macneill, D. Olivito, S. Padhi, M. Pieri, M. Sani, V. Sharma, S. Simon, M. Tadel, A. Vartak, S. Wasserbaech[64], C. Welke, J. Wood, F. Würthwein, A. Yagil, G. Zevi Della Porta

University of California, Santa Barbara - Department of Physics, Santa Barbara, U.S.A.

R. Bhandari, J. Bradmiller-Feld, C. Campagnari, A. Dishaw, V. Dutta, K. Flowers, M. Franco Sevilla, P. Geffert, C. George, F. Golf, L. Gouskos, J. Gran, R. Heller, J. Incandela, N. Mccoll, S.D. Mullin, A. Ovcharova, J. Richman, D. Stuart, I. Suarez, C. West, J. Yoo

California Institute of Technology, Pasadena, U.S.A.

D. Anderson, A. Apresyan, J. Bendavid, A. Bornheim, J. Bunn, Y. Chen, J. Duarte, A. Mott, H.B. Newman, C. Pena, M. Spiropulu, J.R. Vlimant, S. Xie, R.Y. Zhu

Carnegie Mellon University, Pittsburgh, U.S.A.

M.B. Andrews, V. Azzolini, B. Carlson, T. Ferguson, M. Paulini, J. Russ, M. Sun, H. Vogel, I. Vorobiev

University of Colorado Boulder, Boulder, U.S.A.

J.P. Cumalat, W.T. Ford, F. Jensen, A. Johnson, M. Krohn, T. Mulholland, K. Stenson, S.R. Wagner

Cornell University, Ithaca, U.S.A.

J. Alexander, J. Chaves, J. Chu, S. Dittmer, K. Mcdermott, N. Mirman, G. Nicolas Kaufman, J.R. Patterson, A. Rinkevicius, A. Ryd, L. Skinnari, L. Soffi, S.M. Tan, Z. Tao, J. Thom, J. Tucker, P. Wittich, M. Zientek

Fairfield University, Fairfield, U.S.A.

D. Winn

Fermi National Accelerator Laboratory, Batavia, U.S.A.

S. Abdullin, M. Albrow, G. Apollinari, S. Banerjee, L.A.T. Bauerdick, A. Beretvas, J. Berryhill, P.C. Bhat, G. Bolla, K. Burkett, J.N. Butler, H.W.K. Cheung, F. Chlebana, S. Cihangir, M. Cremonesi, V.D. Elvira, I. Fisk, J. Freeman, E. Gottschalk, L. Gray, D. Green, S. Grünendahl, O. Gutsche, D. Hare, R.M. Harris, S. Hasegawa, J. Hirschauer, Z. Hu, B. Jayatilaka, S. Jindariani, M. Johnson, U. Joshi, B. Klima, B. Kreis, S. Lammel, J. Linacre, D. Lincoln, R. Lipton, T. Liu, R. Lopes De Sá, J. Lykken, K. Maeshima, N. Magini, J.M. Marraffino, S. Maruyama, D. Mason, P. McBride, P. Merkel, S. Mrenna, S. Nahn, C. Newman-Holmes[†], V. O'Dell, K. Pedro, O. Prokofyev, G. Rakness, L. Ristori, E. Sexton-Kennedy, A. Soha, W.J. Spalding, L. Spiegel, S. Stoynev, N. Strobbe, L. Taylor, S. Tkaczyk, N.V. Tran, L. Uplegger, E.W. Vaandering, C. Vernieri, M. Verzocchi, R. Vidal, M. Wang, H.A. Weber, A. Whitbeck

University of Florida, Gainesville, U.S.A.

D. Acosta, P. Avery, P. Bortignon, D. Bourilkov, A. Brinkerhoff, A. Carnes, M. Carver, D. Curry, S. Das, R.D. Field, I.K. Furic, J. Konigsberg, A. Korytov, P. Ma, K. Matchev, H. Mei, P. Milenovic[65], G. Mitselmakher, D. Rank, L. Shchutska, D. Sperka, L. Thomas, J. Wang, S. Wang, J. Yelton

Florida International University, Miami, U.S.A.

S. Linn, P. Markowitz, G. Martinez, J.L. Rodriguez

Florida State University, Tallahassee, U.S.A.

A. Ackert, J.R. Adams, T. Adams, A. Askew, S. Bein, B. Diamond, S. Hagopian, V. Hagopian, K.F. Johnson, A. Khatiwada, H. Prosper, A. Santra, M. Weinberg

Florida Institute of Technology, Melbourne, U.S.A.

M.M. Baarmand, V. Bhopatkar, S. Colafranceschi[66], M. Hohlmann, D. Noonan, T. Roy, F. Yumiceva

University of Illinois at Chicago (UIC), Chicago, U.S.A.

M.R. Adams, L. Apanasevich, D. Berry, R.R. Betts, I. Bucinskaite, R. Cavanaugh, O. Evdokimov, L. Gauthier, C.E. Gerber, D.J. Hofman, P. Kurt, C. O'Brien, I.D. Sandoval Gonzalez, P. Turner, N. Varelas, H. Wang, Z. Wu, M. Zakaria, J. Zhang

The University of Iowa, Iowa City, U.S.A.

B. Bilki[67], W. Clarida, K. Dilsiz, S. Durgut, R.P. Gandrajula, M. Haytmyradov, V. Khristenko, J.-P. Merlo, H. Mermerkaya[68], A. Mestvirishvili, A. Moeller, J. Nachtman, H. Ogul, Y. Onel, F. Ozok[69], A. Penzo, C. Snyder, E. Tiras, J. Wetzel, K. Yi

Johns Hopkins University, Baltimore, U.S.A.

I. Anderson, B. Blumenfeld, A. Cocoros, N. Eminizer, D. Fehling, L. Feng, A.V. Gritsan, P. Maksimovic, M. Osherson, J. Roskes, U. Sarica, M. Swartz, M. Xiao, Y. Xin, C. You

The University of Kansas, Lawrence, U.S.A.

A. Al-bataineh, P. Baringer, A. Bean, J. Bowen, C. Bruner, J. Castle, R.P. Kenny III, A. Kropivnitskaya, D. Majumder, W. Mcbrayer, M. Murray, S. Sanders, R. Stringer, J.D. Tapia Takaki, Q. Wang

Kansas State University, Manhattan, U.S.A.

A. Ivanov, K. Kaadze, S. Khalil, M. Makouski, Y. Maravin, A. Mohammadi, L.K. Saini, N. Skhirtladze, S. Toda

Lawrence Livermore National Laboratory, Livermore, U.S.A.

D. Lange, F. Rebassoo, D. Wright

University of Maryland, College Park, U.S.A.

C. Anelli, A. Baden, O. Baron, A. Belloni, B. Calvert, S.C. Eno, C. Ferraioli, J.A. Gomez, N.J. Hadley, S. Jabeen, R.G. Kellogg, T. Kolberg, J. Kunkle, Y. Lu, A.C. Mignerey, Y.H. Shin, A. Skuja, M.B. Tonjes, S.C. Tonwar

Massachusetts Institute of Technology, Cambridge, U.S.A.

D. Abercrombie, B. Allen, A. Apyan, R. Barbieri, A. Baty, R. Bi, K. Bierwagen, S. Brandt, W. Busza, I.A. Cali, Z. Demiragli, L. Di Matteo, G. Gomez Ceballos, M. Goncharov, D. Hsu, Y. Iiyama, G.M. Innocenti, M. Klute, D. Kovalskyi, K. Krajczar, Y.S. Lai, Y.-J. Lee, A. Levin, P.D. Luckey, A.C. Marini, C. Mcginn, C. Mironov, S. Narayanan, X. Niu, C. Paus, C. Roland, G. Roland, J. Salfeld-Nebgen, G.S.F. Stephans, K. Sumorok, K. Tatar, M. Varma, D. Velicanu, J. Veverka, J. Wang, T.W. Wang, B. Wyslouch, M. Yang, V. Zhukova

University of Minnesota, Minneapolis, U.S.A.

A.C. Benvenuti, R.M. Chatterjee, A. Evans, A. Finkel, A. Gude, P. Hansen, S. Kalafut, S.C. Kao, Y. Kubota, Z. Lesko, J. Mans, S. Nourbakhsh, N. Ruckstuhl, R. Rusack, N. Tambe, J. Turkewitz

University of Mississippi, Oxford, U.S.A.

J.G. Acosta, S. Oliveros

University of Nebraska-Lincoln, Lincoln, U.S.A.

E. Avdeeva, R. Bartek, K. Bloom, S. Bose, D.R. Claes, A. Dominguez, C. Fangmeier, R. Gonzalez Suarez, R. Kamalieddin, D. Knowlton, I. Kravchenko, A. Malta Rodrigues, F. Meier, J. Monroy, J.E. Siado, G.R. Snow, B. Stieger

State University of New York at Buffalo, Buffalo, U.S.A.

M. Alyari, J. Dolen, J. George, A. Godshalk, C. Harrington, I. Iashvili, J. Kaisen, A. Kharchilava, A. Kumar, A. Parker, S. Rappoccio, B. Roozbahani

Northeastern University, Boston, U.S.A.

G. Alverson, E. Barberis, D. Baumgartel, A. Hortiangtham, A. Massironi, D.M. Morse, D. Nash, T. Orimoto, R. Teixeira De Lima, D. Trocino, R.-J. Wang, D. Wood

Northwestern University, Evanston, U.S.A.

S. Bhattacharya, K.A. Hahn, A. Kubik, J.F. Low, N. Mucia, N. Odell, B. Pollack, M.H. Schmitt, K. Sung, M. Trovato, M. Velasco

University of Notre Dame, Notre Dame, U.S.A.

N. Dev, M. Hildreth, K. Hurtado Anampa, C. Jessop, D.J. Karmgard, N. Kellams, K. Lannon, N. Marinelli, F. Meng, C. Mueller, Y. Musienko[35], M. Planer, A. Reinsvold, R. Ruchti, G. Smith, S. Taroni, N. Valls, M. Wayne, M. Wolf, A. Woodard

The Ohio State University, Columbus, U.S.A.

J. Alimena, L. Antonelli, J. Brinson, B. Bylsma, L.S. Durkin, S. Flowers, B. Francis, A. Hart, C. Hill, R. Hughes, W. Ji, B. Liu, W. Luo, D. Puigh, B.L. Winer, H.W. Wulsin

Princeton University, Princeton, U.S.A.

S. Cooperstein, O. Driga, P. Elmer, J. Hardenbrook, P. Hebda, J. Luo, D. Marlow, T. Medvedeva, M. Mooney, J. Olsen, C. Palmer, P. Piroué, D. Stickland, C. Tully, A. Zuranski

University of Puerto Rico, Mayaguez, U.S.A.

S. Malik

Purdue University, West Lafayette, U.S.A.

A. Barker, V.E. Barnes, D. Benedetti, S. Folgueras, L. Gutay, M.K. Jha, M. Jones, A.W. Jung, K. Jung, D.H. Miller, N. Neumeister, B.C. Radburn-Smith, X. Shi, J. Sun, A. Svyatkovskiy, F. Wang, W. Xie, L. Xu

Purdue University Calumet, Hammond, U.S.A.

N. Parashar, J. Stupak

Rice University, Houston, U.S.A.

A. Adair, B. Akgun, Z. Chen, K.M. Ecklund, F.J.M. Geurts, M. Guilbaud, W. Li, B. Michlin, M. Northup, B.P. Padley, R. Redjimi, J. Roberts, J. Rorie, Z. Tu, J. Zabel

University of Rochester, Rochester, U.S.A.

B. Betchart, A. Bodek, P. de Barbaro, R. Demina, Y.t. Duh, T. Ferbel, M. Galanti, A. Garcia-Bellido, J. Han, O. Hindrichs, A. Khukhunaishvili, K.H. Lo, P. Tan, M. Verzetti

Rutgers, The State University of New Jersey, Piscataway, U.S.A.

J.P. Chou, E. Contreras-Campana, Y. Gershtein, T.A. Gómez Espinosa, E. Halkiadakis, M. Heindl, D. Hidas, E. Hughes, S. Kaplan, R. Kunnawalkam Elayavalli, S. Kyriacou,

A. Lath, K. Nash, H. Saka, S. Salur, S. Schnetzer, D. Sheffield, S. Somalwar, R. Stone, S. Thomas, P. Thomassen, M. Walker

University of Tennessee, Knoxville, U.S.A.

M. Foerster, J. Heideman, G. Riley, K. Rose, S. Spanier, K. Thapa

Texas A&M University, College Station, U.S.A.

O. Bouhali[70], A. Celik, M. Dalchenko, M. De Mattia, A. Delgado, S. Dildick, R. Eusebi, J. Gilmore, T. Huang, E. Juska, T. Kamon[71], R. Mueller, Y. Pakhotin, R. Patel, A. Perloff, L. Perniè, D. Rathjens, A. Rose, A. Safonov, A. Tatarinov, K.A. Ulmer

Texas Tech University, Lubbock, U.S.A.

N. Akchurin, C. Cowden, J. Damgov, C. Dragoiu, P.R. Dudero, J. Faulkner, S. Kunori, K. Lamichhane, S.W. Lee, T. Libeiro, S. Undleeb, I. Volobouev, Z. Wang

Vanderbilt University, Nashville, U.S.A.

A.G. Delannoy, S. Greene, A. Gurrola, R. Janjam, W. Johns, C. Maguire, A. Melo, H. Ni, P. Sheldon, S. Tuo, J. Velkovska, Q. Xu

University of Virginia, Charlottesville, U.S.A.

M.W. Arenton, P. Barria, B. Cox, J. Goodell, R. Hirosky, A. Ledovskoy, H. Li, C. Neu, T. Sinthuprasith, X. Sun, Y. Wang, E. Wolfe, F. Xia

Wayne State University, Detroit, U.S.A.

C. Clarke, R. Harr, P.E. Karchin, P. Lamichhane, J. Sturdy

University of Wisconsin - Madison, Madison, WI, U.S.A.

D.A. Belknap, S. Dasu, L. Dodd, S. Duric, B. Gomber, M. Grothe, M. Herndon, A. Hervé, P. Klabbers, A. Lanaro, A. Levine, K. Long, R. Loveless, I. Ojalvo, T. Perry, G.A. Pierro, G. Polese, T. Ruggles, A. Savin, A. Sharma, N. Smith, W.H. Smith, D. Taylor, N. Woods

†: Deceased
1: Also at Vienna University of Technology, Vienna, Austria
2: Also at State Key Laboratory of Nuclear Physics and Technology, Peking University, Beijing, China
3: Also at Institut Pluridisciplinaire Hubert Curien, Université de Strasbourg, Université de Haute Alsace Mulhouse, CNRS/IN2P3, Strasbourg, France
4: Also at Universidade Estadual de Campinas, Campinas, Brazil
5: Also at Université Libre de Bruxelles, Bruxelles, Belgium
6: Also at Deutsches Elektronen-Synchrotron, Hamburg, Germany
7: Also at Joint Institute for Nuclear Research, Dubna, Russia
8: Now at British University in Egypt, Cairo, Egypt
9: Also at Zewail City of Science and Technology, Zewail, Egypt
10: Now at Fayoum University, El-Fayoum, Egypt
11: Now at Ain Shams University, Cairo, Egypt
12: Also at Université de Haute Alsace, Mulhouse, France
13: Also at CERN, European Organization for Nuclear Research, Geneva, Switzerland
14: Also at Skobeltsyn Institute of Nuclear Physics, Lomonosov Moscow State University, Moscow, Russia

15: Also at Tbilisi State University, Tbilisi, Georgia

16: Also at RWTH Aachen University, III. Physikalisches Institut A, Aachen, Germany

17: Also at University of Hamburg, Hamburg, Germany

18: Also at Brandenburg University of Technology, Cottbus, Germany

19: Also at Institute of Nuclear Research ATOMKI, Debrecen, Hungary

20: Also at MTA-ELTE Lendület CMS Particle and Nuclear Physics Group, Eötvös Loránd University, Budapest, Hungary

21: Also at University of Debrecen, Debrecen, Hungary

22: Also at Indian Institute of Science Education and Research, Bhopal, India

23: Also at Institute of Physics, Bhubaneswar, India

24: Also at University of Visva-Bharati, Santiniketan, India

25: Also at University of Ruhuna, Matara, Sri Lanka

26: Also at Isfahan University of Technology, Isfahan, Iran

27: Also at University of Tehran, Department of Engineering Science, Tehran, Iran

28: Also at Plasma Physics Research Center, Science and Research Branch, Islamic Azad University, Tehran, Iran

29: Also at Università degli Studi di Siena, Siena, Italy

30: Also at Purdue University, West Lafayette, U.S.A.

31: Also at International Islamic University of Malaysia, Kuala Lumpur, Malaysia

32: Also at Malaysian Nuclear Agency, MOSTI, Kajang, Malaysia

33: Also at Consejo Nacional de Ciencia y Tecnología, Mexico city, Mexico

34: Also at Warsaw University of Technology, Institute of Electronic Systems, Warsaw, Poland

35: Also at Institute for Nuclear Research, Moscow, Russia

36: Now at National Research Nuclear University 'Moscow Engineering Physics Institute' (MEPhI), Moscow, Russia

37: Also at St. Petersburg State Polytechnical University, St. Petersburg, Russia

38: Also at University of Florida, Gainesville, U.S.A.

39: Also at P.N. Lebedev Physical Institute, Moscow, Russia

40: Also at California Institute of Technology, Pasadena, U.S.A.

41: Also at Faculty of Physics, University of Belgrade, Belgrade, Serbia

42: Also at INFN Sezione di Roma; Università di Roma, Roma, Italy

43: Also at National Technical University of Athens, Athens, Greece

44: Also at Scuola Normale e Sezione dell'INFN, Pisa, Italy

45: Also at National and Kapodistrian University of Athens, Athens, Greece

46: Also at Riga Technical University, Riga, Latvia

47: Also at Institute for Theoretical and Experimental Physics, Moscow, Russia

48: Also at Albert Einstein Center for Fundamental Physics, Bern, Switzerland

49: Also at Gaziosmanpasa University, Tokat, Turkey

50: Also at Adiyaman University, Adiyaman, Turkey

51: Also at Mersin University, Mersin, Turkey

52: Also at Cag University, Mersin, Turkey

53: Also at Piri Reis University, Istanbul, Turkey

54: Also at Ozyegin University, Istanbul, Turkey

55: Also at Izmir Institute of Technology, Izmir, Turkey

56: Also at Marmara University, Istanbul, Turkey

57: Also at Kafkas University, Kars, Turkey

58: Also at Istanbul Bilgi University, Istanbul, Turkey

59: Also at Yildiz Technical University, Istanbul, Turkey

60: Also at Hacettepe University, Ankara, Turkey

61: Also at Rutherford Appleton Laboratory, Didcot, United Kingdom

62: Also at School of Physics and Astronomy, University of Southampton, Southampton, United Kingdom

63: Also at Instituto de Astrofísica de Canarias, La Laguna, Spain

64: Also at Utah Valley University, Orem, U.S.A.

65: Also at University of Belgrade, Faculty of Physics and Vinca Institute of Nuclear Sciences, Belgrade, Serbia

66: Also at Facoltà Ingegneria, Università di Roma, Roma, Italy

67: Also at Argonne National Laboratory, Argonne, U.S.A.

68: Also at Erzincan University, Erzincan, Turkey

69: Also at Mimar Sinan University, Istanbul, Istanbul, Turkey

70: Also at Texas A&M University at Qatar, Doha, Qatar

71: Also at Kyungpook National University, Daegu, Korea